

Developmental plasticity enables an intestinal tapeworm to adapt to dietary stress

Received: 2 March 2025

Accepted: 2 February 2026

Cite this article as: Jirků, M., Parker, W., Kadlecová, O. *et al.*

Developmental plasticity enables an intestinal tapeworm to adapt to dietary stress. *Nat Commun* (2026). <https://doi.org/10.1038/s41467-026-69475-0>

Milan Jirků, William Parker, Oldřiška Kadlecová, Martin Moos, Monika M. Wiśniewska, Roman Kuchta, Petra Tláskalová, Vladislav Ilík, Aleš Tomčala, Zuzana Pavlíčková, Kristýna Brožová, Julius Lukeš, Miroslav Oborník, Martin Kolísko, Barbora Pafčo & Kateřina Jirků

We are providing an unedited version of this manuscript to give early access to its findings. Before final publication, the manuscript will undergo further editing. Please note there may be errors present which affect the content, and all legal disclaimers apply.

If this paper is publishing under a Transparent Peer Review model then Peer Review reports will publish with the final article.

Developmental plasticity enables an intestinal tapeworm to adapt to dietary stress

Milan Jirků^{1#}, William Parker^{2#}, Oldřiška Kadlecová¹, Martin Moos^{3,4}, Monika M. Wiśniewska^{1,5}, Roman Kuchta¹, Petra Tláskalová^{1,5}, Vladislav Ilík⁶, Aleš Tomčala⁷, Zuzana Pavlíčková¹, Kristýna Brožová¹, Julius Lukeš^{1,5}, Miroslav Oborník^{1,5}, Martin Kolísko^{1,5}, Barbora Pafčo^{6†}, Kateřina Jirků^{1**†}

¹*Institute of Parasitology, Biology Centre, Czech Academy of Sciences, 370 05 České Budějovice, Czech Republic*

²*Department of Surgery, Duke University Medical Center, NC 27710, Durham, USA*

³*Institute of Entomology, Biology Centre, Czech Academy of Sciences, 370 05 České Budějovice, Czech Republic*

⁴*Department of Applied Chemistry, University of South Bohemia, 370 05 České Budějovice, Czech Republic*

⁵*Faculty of Science, University of South Bohemia, 370 05 České Budějovice, Czech Republic*

⁶*Institute of Vertebrate Biology, Czech Academy of Sciences, 603 65 Brno, Czech Republic*

⁷*Institute of Aquaculture and Protection of Waters, 370 05 České Budějovice, CENAKVA FFPW USB, Czech Republic*

*Correspondence

Kateřina Jirků, Institute of Parasitology, Biology Centre, the Czech Academy of Sciences, Branišovská 31, 370 05 České Budějovice, Czech Republic; phone: +420-38-777-5470; email: pomajbikova@paru.cas.cz

#These authors contributed equally

†These authors jointly supervised this work

ABSTRACT

Diet is one of the strongest ecological forces shaping the gut environment, yet its impact on intestinal worms (helminths) remains poorly understood. The helminth *Hymenolepis diminuta* is a suitable model for investigating how lifestyle changes in modern societies may disrupt host–helminth relationships. Here we show that dietary fiber availability shapes the developmental trajectory and life strategies of *H. diminuta* in a stage-dependent manner. Fiber deprivation at the time of host colonization leads to developmental arrest, manifested by reduced growth, absence of reproduction, and transcriptional changes consistent with suppressed development. This state is accompanied by diet-dependent remodeling of the host small intestinal microbiota and metabolome: whereas fiber-rich diets support fermentative microbial communities and a chemically diverse intestinal environment, the Western diet promotes dysbiotic profiles with reduced fermentation capacity and a more pro-inflammatory immune response. In contrast, adult *H. diminuta* that reach maturity in hosts maintained on a fiber-rich diet exhibit a reversible, aestivation-like suppression of reproduction during short-term fiber deprivation, with full restoration of egg production following dietary recovery. Together, these findings indicate that dietary transitions associated with industrialized lifestyles can redirect helminth developmental programs and host–helminth–microbiome interactions, with implications for helminth persistence and potential therapeutic applications.

KEY WORDS

helminth; *Hymenolepis diminuta*; Western diet; arrested development; quiescence; transcriptomics; gut microbiota; metabolomics; helminth-host interactions

INTRODUCTION

The gut is a complex ecosystem where the host coexists with a wide array of microbial and macrobiotic symbionts¹. While research has long focused on bacteria, the gut community also harbors viruses, archaea, fungi, protists, and, in some cases, multicellular eukaryotes such as helminths^{2–5}. These often-overlooked members are now recognized as integral to intestinal ecology, able to reshape microbial balance and modulate host immunity through distinct metabolic and immunological pathways^{2,6}.

Intestinal helminths are increasingly recognized as macro-symbionts with strong immunomodulatory capacity. Once a routine part of the human gut ecosystem, they have largely vanished from Western populations⁷. Their presence can reshape both immunity and bacterial communities, often enriching beneficial Clostridia groups while suppressing pro-inflammatory taxa such as *Bacteroides* and Proteobacteria². Helminths, microbiota, and the host immune system operate as an interdependent network, where the impact of each partner depends on the others⁸. Crucially, specific bacterial taxa can amplify or dampen helminth-driven immune regulation, revealing the bidirectional and context-dependent nature of these interactions^{9,10}.

The decline in helminths is widely attributed to improved sanitation, urbanization, and mass anthelmintic use^{5,11,12}. However, shifts in dietary patterns may also play a decisive role by altering the ecological conditions required for their persistence. Western diets, typically low in microbe-accessible fiber, drive profound changes in gut fermentation profiles and substrate availability, potentially impairing the survival of eukaryotic symbionts^{13,14}. While dietary effects on bacterial communities are well documented, the consequences of host diet for non-bacterial gut residents – particularly helminths – have been explored only in a limited and system-specific way. Emerging studies indicate that diet can influence helminth persistence and developmental outcomes, including tendencies toward hypobiosis^{15–17}, yet this work remains in its early stages and confined to specific experimental systems. Thus, the effects of complex diets on helminth development *in vivo* are still only partly understood.

In addition, modern diets alter key physicochemical parameters of the gut—such as luminal pH, oxygen (redox) gradients, mucus architecture and transit time—that define ecological niches. These features shape microbial composition and activity across intestinal regions^{18,19}. Experimental work further shows that dietary context profoundly reconfigures community assembly, keystone functions and metabolic outputs, with strain–strain relationships and pH modifications varying across carbohydrate environments¹⁹. Such nutritional selection pressures likely drive microbial evolutionary shifts under Westernized conditions¹⁴ and may contribute, together with other aspects of modernization, to the

documented decline of some intestinal eukaryotic symbionts, including helminths, in industrialized populations^{3,7}.

This renewed ecological perspective has also revealed how helminths, through reshaping host-associated microbial networks, modulate immune and metabolic outcomes in ways that can protect against diet-induced pathology²⁰. The rat tapeworm *Hymenolepis diminuta* is among the most promising model helminth, combining potent immunomodulatory and anti-inflammatory effects with low pathogenicity, a well-defined life cycle, and ease of laboratory maintenance^{5,21}. Preclinical studies show protective effects against chemically induced inflammation, allergies, neuroinflammation, and behavioral disorders^{21–24}. In rats, colonization alleviates colitis, reduces expression of *Il1b* and *Tnf*, increases *Il10*, and promotes mucosal repair²³, while shifting the microbiota toward an anti-inflammatory profile, yet these changes are reversed upon decolonization^{9,25–27}. Case reports of self-treatment for conditions such as Inflammatory Bowel Disease, migraines, and ADHD report good safety and tolerance^{21,28,29}.

Yet, therapeutic efficacy is inconsistent, shaped by microbiota composition, inflammatory state, and dietary context. Antibiotic treatment abolishes these benefits⁹, underscoring the role of host–microbiota–helminth interactions⁸. Diet emerges as a key modulator, influencing both gut ecology and helminth development. From an evolutionary perspective, fiber-depleted industrial diets may have imposed selective pressures contributing to the disappearance of eukaryotic gut symbionts^{13,21}. Early experimental work showed that *H. diminuta* physiology can respond to nutritional conditions, but these studies relied mainly on isolated nutrients and simplified settings³⁰.

Here, we show that dietary composition is a critical determinant of the development, physiology, and persistence of the intestinal tapeworm *H. diminuta*. By comparing a Western-type diet rich in fat and refined sugar but lacking microbe-accessible fiber with a complex, fiber-rich diet, we demonstrate that fiber deprivation profoundly constrains tapeworm growth, reproductive maturation, and transcriptional activity. These diet-dependent effects coincide with marked restructuring of the host gut ecosystem, indicating that modern low-fiber dietary patterns destabilize long-standing host–helminth ecological relationships. Together, our findings identify dietary fiber as a key ecological factor governing the viability and functional integration of gut-resident eukaryotic symbionts.

RESULTS

Diet-driven plasticity in tapeworm development

Experiment 1 (Fig. 1A), which tested the effect of host diet on the development of *Hymenolepis diminuta*, revealed marked diet-dependent differences in helminth morphology and reproductive output. Rats were inoculated after diet change on day 30 (Fig. 1A). Tapeworms from rats maintained on the Accessible Fiber diet exhibited a normal colonization rate (100%; $n = 16$) and fully mature morphology, characterized by normal length (i.e., 20–60 cm in rats), fully developed copulatory organs, and egg-filled uteri in the posterior proglottids (Fig. 2A, C, E). In contrast, *H. diminuta* recovered from rats on the Western (fiber-free) diet showed a reduced colonization rate (50%; 16 out of total 32 rats) and arrested development, displaying an immature phenotype (Fig. 2B, D). Among colonized hosts, tapeworms from Western-diet rats were dramatically shorter and undeveloped than those from Accessible Fiber fed rats (Western diet: 2.69 ± 1.41 cm, $n = 16$; Accessible Fiber diet: 20.81 ± 2.74 cm, $n = 16$; mean difference = 18.13 ± 0.77 cm 95% CI [16.53, 19.72]; Welch's t-test, $t(22) = 23.49$, $p < 0.0001$, $\eta^2 = 0.96$) (Fig. 2F; Source data are available on Figshare DOI: XXXX).

Using Sheather's flotation, *H. diminuta* eggs were detected in the feces of rats maintained on the Accessible Fiber diet, whereas no eggs were found in those on the Western diet during the patent period (i.e., ≥ 20 days post-colonization, when adult tapeworms are typically fully developed). Unexpectedly, necropsy on day 60 (i.e., 30 days post-inoculation) consistently revealed the presence of immature tapeworms in Western-diet rats. Further morphological evaluation confirmed arrested development, with posterior proglottids containing only immature reproductive organs and lacking a developed uterus (Fig. 2B, D).

For clarity, colonization is defined here as the presence of *H. diminuta* in the host gut, irrespective of reproductive activity. In rats fed the Accessible Fiber diet, colonization was confirmed by egg shedding, whereas in rats on the Western diet no eggs were detected, but endpoint necropsies consistently revealed stunted immature tapeworms. Thus, the definition of colonization was consistent across groups, while the method of confirmation differed depending on diet.

Experiment 2 (Fig. 1B) tested whether the reproductive effects of a temporary Western diet exposure are reversible in adult tapeworms. A 90-day experiment with three dietary regimens was conducted, with all rats initially colonized on the Accessible Fiber diet ($n = 6$ per group; total $n = 18$); the diet shift was introduced when patency was confirmed (Fig. 1B). Egg output was monitored throughout and revealed that reproductive activity can indeed be restored by dietary manipulation. In the experimental recovery

group, colonized rats were first maintained on the Accessible Fiber diet for 50 days (30 days of exposure plus a 20-day prepatent period), then switched to the Western, fiber-free diet for 10 days, and finally returned to the original fiber-rich diet for 30 days (Fig. 3).

Rats kept continuously on the Accessible Fiber diet maintained high and stable egg counts during the patent period (egg counts between days 21 and 50: 999.7 ± 82.95 eggs/g feces). Switching to the Western diet on day 50 triggered a rapid decline, culminating in complete cessation of egg shedding by day 55. Reintroduction of the Accessible Fiber diet restored egg production on between days 73-75 (egg counts from day 73 - 251.8 ± 71.34 eggs/g during recovery), with all returning rats resuming egg shedding at levels approaching those of continuous control group (egg counts from day 73 - 737.8 ± 55.54 eggs/g), indicating recovery of reproductive capacity (Fig. 3). In contrast, rats maintained on the Western diet from day 50 until the end of experiment exhibited egg count 0.

Repeated-measures negative binomial generalized linear modeling revealed a strong group \times time interaction ($\chi^2(2) = 290.83$, FDR-adjusted $p < 0.001$) in all groups ($n = 6$ per group). The Accessible Fiber group showed stable egg output over time (slope = -0.00332 eggs/day, 95% CI [$-0.01299, 0.00635$]), while both groups exposed to the Western diet exhibited steep declines (Western diet: slope = -0.20480 , 95% CI [$-0.22832, -0.18128$]; recovery group during Western diet: slope = -0.03617 , 95% CI [$-0.04434, -0.02801$]). Following fiber reintroduction, egg production resumed in this group as indicated by a significantly attenuated temporal decline relative to the Western diet group (slope = 0.16862 , 95% CI [$0.14379, 0.19346$], $Z = 13.31$, $p < 1 \times 10^{-10}$; Fig. 3).

Transient fluctuations in egg counts during days 25–35 resulted in some early statistical differences; however, these occurred while all rats were maintained on the same diet and were therefore not considered biologically meaningful. Following dietary transitions, significant differences between the continuous Accessible Fiber group and both the Western and recovery groups on days 54–57 (model-based contrasts: $Z = 3.1$ – 6.1 , FDR-adjusted $p < 0.001$). During the recovery phase, egg counts in the recovery group remained significantly lower than those of the continuous Accessible Fiber group on days 73 and 75 ($Z = 4.2$ – 4.7 , FDR-adjusted $p < 0.001$), reflecting the delayed resumption of egg production (Fig. 3).

Within-group analyses using the same modeling framework supported these findings: egg output remained stable in the continuous Accessible Fiber group (all comparisons $p > 0.35$), declined rapidly and did not recover within the experimental timeframe under the Western diet ($p < 0.001$), and was restored after fiber reintroduction (recovery group: significant reduction during Western diet, $p < 0.001$; recovery to pre-transition levels, $p = 0.50$; Fig. 3; Source data are available on Figshare DOI: XXXX).

Transcriptomic adaptations of tapeworm to dietary stress

Comparative transcriptomic profiling of *H. diminuta*, performed on three biological replicates per dietary group, identified pronounced diet-associated differences in gene expression between tapeworms recovered from rats fed the Western (fiber-free) diet and those fed the Accessible Fiber diet. Using a conservative threshold (FDR < 0.01, $|\log_2FC| > 1$), we detected 691 upregulated and 786 downregulated genes in tapeworms from the Western diet group relative to the Accessible Fiber diet group (Fig. 4 and Supplementary Figs. 1–3).

Specifically, genes showing reduced expression under the Western diet were enriched for functional categories associated with multicellular organism development, including components of the WNT signaling pathway (9 genes; Supplementary Fig. 4), as well as genes involved in mitosis and meiosis (*zyg-11*, 25 centrosome components and 3 recombination nodule components) (Supplementary Data 1). In addition, reduced expression was also observed for genes annotated to muscle function (e.g., myosin metabolism; 4 genes) and energy metabolism pathways (e.g., glucose metabolism; 2 genes). Conversely, genes with relatively higher expression in tapeworms from Western diet were enriched for purine and pyrimidine metabolism (11 genes), transmembrane transporter activity (17 genes), and cell–cell junctions (16 genes) (Supplementary Fig. 1).

Genes related to cellular stress responses were also differentially expressed. Thirteen genes were annotated as oxidative stress regulation, detoxification, and mitochondrial signaling. These include genes related to the modulation of reactive oxygen species (ROS), such as voltage-gated proton channel genes (two upregulated, three downregulated) and cytochrome b5 reductase genes (two upregulated). Detoxification-associated genes with glutathione transferase activity were downregulated (five genes), and the tryptophan-rich sensory protein (*tsp*) gene, a homolog of the mitochondrial benzodiazepine receptor, was also downregulated (Supplementary Data 1).

Small intestinal microbiota shaped by diet and tapeworm

Microbiome analyses showed that diet dominated small intestinal communities, whereas effects of *H. diminuta* were subtle and diet dependent. The total number of reads after quality filtering was 5,407,746 (min = 74,053; max = 153,034; median = 111,752), which clustered into 4,180 ASVs. Rats fed the Accessible Fiber diet showed significant enrichment of bacterial taxa typically associated with gut homeostasis and beneficial metabolic activity, such as fiber fermentation. These included members of the order Lactobacillales, such as *Lactobacillus*, *Ligilactobacillus*, and *Limosilactobacillus*, as well as *Turicibacter* and

taxa within the order Erysipelotrichales (Fig. 5A). In contrast, the Western diet promoted the expansion of multiple taxa linked to dysbiosis and host stress, including genera such as *Streptococcus*, *Staphylococcus*, *Clostridium sensu stricto 1*, and *Romboutsia*, affiliated with the orders Clostridiales, Staphylococcales, Burkholderiales, and Peptostreptococcales–Tissierellales (Fig. 5A).

LEfSe analysis further revealed that shifts associated with *H. diminuta* colonization were strongly diet-dependent, with no enriched taxa detected in colonized rats under the fiber-rich diet (Fig. 5B), while helminth colonization under the Western diet modulated microbiota structure, enriching for representatives within potentially pathogenic Clostridiales (Fig. 5C).

Alpha diversity analyses revealed that the Western diet was associated with significantly lower microbial diversity compared to the Accessible Fiber diet (GLM_richness: $t(28) = -4.02$, $p = 0.0004$, $\beta = -380.0$, 95% CI [-573.8, -186.2]; GLM_Simpson: $t(30) = -2.73$, $p = 0.010$, $\beta = -0.099$, 95% CI [-0.172, -0.025]), regardless of colonization status (Fig. 6A–B). In line with these findings, beta diversity analyses revealed clear clustering by diet (Fig. 6C–D). Both Bray–Curtis and Jaccard metrics showed significant separation between the microbial communities of rats fed the Accessible Fiber versus the Western diet (ANOSIM_Bray: $R = 0.8683$, permutations = 999 $p = 0.001$; ANOSIM_Jaccard: $R = 0.781$, permutations = 999, $p = 0.001$). These results emphasize the dominant role of dietary composition in shaping microbiota structure.

When analyzing the effect of *H. diminuta* colonization, no significant differences in alpha diversity were detected (GLM_richness: $t(30) = -0.43$, $p = 0.743$, $\beta = -42.6$, 95% CI [-247.5, 162.3]; GLM_Simpson: $t(30) = 0.75$, $p = 0.766$, $\beta = 0.030$, 95% CI [-0.052, 0.112]; Fig. 7A–B). However, colonization altered microbial community composition, particularly under the Western diet. In rats fed the Accessible Fiber diet, modest but partially significant differences—explaining a relatively small proportion of the variability—were observed between colonized and non-colonized groups (ANOSIM_Bray: $R = 0.1083$, permutations = 999, $p = 0.053$; ANOSIM_Jaccard: $R = 0.1629$, permutations = 999, $p = 0.024$; Fig. 7A–B). These effects were considerably more pronounced under the Western diet, where colonization induced marked shifts in microbial composition (ANOSIM_Bray: $R = 0.1981$, permutations = 999 $p = 0.02$; ANOSIM_Jaccard: $R = 0.4528$, $p = 0.004$; Fig. 7C–D). This pattern highlights the greater sensitivity of Western diet-associated microbiota to external perturbations such as tapeworm colonization.

Intestinal metabolome driven primarily by dietary composition

Diet had a strong effect on the small intestinal metabolome (Fig. 8). Principal component analysis (PCA) shows a robust separation of the examined metabolomes and confirms that the impact of diet is a key

factor; on the other hand, the presence of *H. diminuta* seems to have a marginal influence. This was confirmed by redundancy analysis (RDA) of key metabolites (Monte Carlo test - 999 unrestricted permutations under the reduced model), which revealed a clear separation between rats fed the Accessible Fiber diet and those on the Western diet. The first canonical axis was highly significant (eigenvalue = 0.525, $F = 31.999$, $p = 0.0010$). Likewise, the overall test of all canonical axes (Trace = 0.561) demonstrated significant multivariate structure ($F = 18.563$, $p = 0.0010$). RDA1 is explaining 93.4 % and RDA2 explaining 6.6 % of the variance (Fig. 8A). Fructose was detected exclusively in the Western diet group and was the top discriminating metabolite, whereas the Accessible Fiber group was characterized by unique metabolites such as trihydroxylinoleic acid, 2R-hydroperoxylinoleic acid, hydroperoxy-octadecatrienoic acid, pipercolic acid betaine, and other small organic acids.

Focused PCAs on individual diet groups revealed a diet-dependent impact of *H. diminuta* colonization (Fig. 8C–D). With the Accessible Fiber diet, colonization produced a clear separation between groups, with PC1 explaining 29.6 % and PC2 explaining 25.6 % of the variance (Fig. 8C). This separation was driven by the consistent presence of specific diacylglycerols and amino acids in colonized animals that were absent in non-colonized controls. In contrast, for the Western diet group, PCA showed partial overlap between colonized and non-colonized animals, with PC1 and PC2 explaining 20.7 % and 28.1 % of the variance, respectively (Fig. 8D; Source data and Metabolite annotation summary are available on Figshare DOI: XXXX).

Host-helminth interactions conditioned by diet

Diet strongly shaped the cytokine response to *H. diminuta* colonization (Fig. 9). Expression of the anti-inflammatory cytokines *Il4* and *Il13* differed significantly among experimental groups (Kruskal–Wallis: *Il4* - $H(3) = 18.62$, $p = 0.0003$, $\epsilon^2 = 0.56$; *Il13* - $H(3) = 21.48$, $p < 0.0001$, $\epsilon^2 = 0.66$). Both cytokines were upregulated in colonized rats fed the Accessible Fiber diet compared with non-colonized Accessible Fiber controls (*Il4*: $Z = 3.198$, adjusted $p = 0.0083$; *Il13*: $Z = 3.600$, adjusted $p = 0.0019$). In Accessible Fiber–colonized rats, *Il4* expression was also higher than in both Western-diet groups (colonized Western: $Z = 3.01$, adjusted $p = 0.0156$; non-colonized Western: $Z = 4.02$, adjusted $p = 0.0003$), whereas *Il13* differed only relative to non-colonized Western rats ($Z = 4.21$, adjusted $p = 0.0002$).

For the pro-inflammatory cytokines *Ifng* and *Il1b*, expression differed significantly among groups (Kruskal–Wallis: *Ifng* - $H(3) = 18.20$, $p = 0.0004$, $\epsilon^2 = 0.54$; *Il1b* - $H(3) = 17.89$, $p = 0.0005$, $\epsilon^2 = 0.53$). *Ifng* was specifically elevated in colonized rats on the Western diet compared with non-colonized Western controls ($Z = 3.91$, adjusted $p = 0.0006$) and both Accessible Fiber groups (colonized: $Z = 2.85$, adjusted p

= 0.0261; non-colonized: $Z = 3.37$, adjusted $p = 0.0045$). In contrast, Il1b expression was significantly reduced in colonized rats fed the Accessible Fiber diet compared with non-colonized Accessible Fiber controls ($Z = 3.27$, adjusted $p = 0.0066$) as well as both Western-diet groups (non-colonized: $Z = 3.79$, adjusted $p = 0.0009$; colonized: $Z = 3.19$, adjusted $p = 0.0087$). Source data for Fig. 9 are available on Figshare DOI: XXXX.

Body-weight analysis revealed a strong main effect of diet, with rats fed a Western diet gaining more weight than those fed the Accessible Fiber diet (Three-way repeated measures ANOVA; main effect of diet: $F(1, 28) = 99.0$; $p < 0.001$, $\eta^2 = 0.139$; Supplementary Fig. 5A). Colonization also exerted a significant overall effect on body weight (main effect of colonization: $F(1, 28) = 17.0$; $p = 0.0002$, $\eta^2 = 0.025$). A strong main effect of time was observed ($F(3.112, 87.13) = 39.0$; $p = 0.0001$, $\eta^2 = 0.721$), and both factors showed significant time-dependent effects (time \times diet: $F(3.112, 87.13) = 18.3$, $p = 0.0001$, $\eta^2 = 0.03$; time \times colonization: $F(3.112, 87.13) = 6.0$, $p = 0.0001$, $\eta^2 = 0.01$). Post-hoc analyses showed that under the Western diet group, colonized rats exhibited a steeper weight-gain trajectory than non-colonized controls from day 30 onwards (Tukey's multiple comparisons test; $p < 0.01$ – 0.001 across significant days; Supplementary Fig. 5C). Under the Accessible Fiber diet, colonization was associated with a modest increase in body weight, reaching statistical significance only at later stages (Tukey's multiple comparisons test; $p < 0.05$ – 0.01 ; Supplementary Fig. 5B). Source data for Supplementary data 5 are available on Figshare DOI: XXXX.

DISCUSSION

The ability to survive adverse conditions is widespread among invertebrates, using strategies such as aestivation, diapause, quiescence, and metabolic dormancy^{31–33}. These nutrient-responsive states slow metabolism and halt development through major shifts in gene expression³⁴. In the model free-living nematode *Caenorhabditis elegans*, such plasticity includes hormonally regulated diapause and nutritionally induced quiescence at both larval and adult stages^{32,35,36}.

Whether parasitic helminths exhibit comparable developmental flexibility is only partly understood, with recent work showing diet-dependent shifts in persistence and larval arrest in specific host–parasite systems^{15–17}. The intestinal tapeworm *Hymenolepis diminuta* is a relevant model due to its capacity to modulate host immunity²³ and potential for use in helminth therapy^{5,21}. Here, we examined its adaptive responses to dietary stress, focusing on how the availability of microbially fermentable fiber affects its development and physiology. We compared two diets with strongly contrasting fiber content.

Early work suggested that *H. diminuta* competes with its host for nutrients, influencing physiology and proglottid formation^{37,38}. Similar diet effects occur in *Trichuris suis*, where inulin—a fermentable fiber—enhanced a Th2-biased immune profile, barrier cell expansion, and an anti-inflammatory microbiota without increasing parasite burden¹⁵. In *Trichuris muris*, however, inulin suppresses Th2 immunity and prolongs infection, whereas resistant starch promoted clearance¹⁶. These findings show how diet composition, fiber type, and parasite species interact to shape helminth performance.

Building on this evidence, our results show that *H. diminuta* can adopt two strategies depending on the developmental stage at the onset of dietary stress. When colonization began on a fiber-poor Western diet (Experiment 1), colonization success dropped from 100% to 50%, and surviving worms exhibited arrested development—reduced body size, absence of egg production, and immature reproductive organs—likely reflecting nutritional stress, a pattern also recently observed in other helminths¹⁷. In Experiment 2, adults matured on a fiber-rich diet exhibited reversible suppression of reproduction during short-term deprivation, resembling quiescence or aestivation, with metabolic downregulation and oviposition arrest^{31,35}. Reproduction resumed after diet restoration, confirming a reversible adjustment. The ability to suspend reproduction for up to 30 days and then fully restore egg output demonstrate the capacity of *H. diminuta* to modulate its life cycle in response to host dietary quality. Whether this reversibility applies to immature tapeworms on the Western diet (Experiment 1) remains unclear and is a topic for future studies. Two scenarios are plausible: (i) arrested tapeworms would mature and begin producing eggs after transfer to a fiber-accessible diet, or (ii) they would remain in stasis despite improved nutrition.

When interpreting these patterns, it is important to note that tapeworms on the Western diet in Experiment 1 did not reach reproductive maturity, so colonization could not be confirmed by fecal egg detection and had to be verified at necropsy. Although these methods differ, both reliably established the presence of *H. diminuta* and therefore do not affect our interpretation of colonization success across diets. Diet-induced suppression of reproduction nevertheless lowers the sensitivity of egg-based diagnostics.

Developmental survival strategies in invertebrates often involve large-scale transcriptional reprogramming that reshapes growth, differentiation, and metabolism^{32,34}. In our study, *H. diminuta* exposed to a Western diet from the onset of colonization (Experiment 1) exhibited transcriptional signatures indicative of diet-induced developmental arrest^{32,39}. Notably, genes associated with reproduction, muscle function, and energy metabolism were markedly downregulated, and reduced expression of meiosis-related and structural protein genes aligned with the absence of egg production and underdeveloped reproductive anatomy, indicating a shift toward a non-reproductive, energy-conserving state. In addition, components of the WNT signaling pathway—central to development and cell differentiation—were both up- and downregulated, reflecting profound developmental changes.

Concurrently, genes linked to stress responses, including ROS regulation and lipid metabolism, were upregulated, indicating activation of protective mechanisms under nutritional challenge. This profile parallels transcriptional programs during Dauer entry in *C. elegans*, a reversible arrest state marked by suppressed growth and metabolic remodeling³⁶. A notable case was the mixed transcriptional response of voltage-gated proton channels (Hv1), with some isoforms upregulated and others downregulated. These channels are key redox regulators whose expression can increase under metabolic stress, particularly in response to saturated fats^{40,41}. In *H. diminuta* from the Western diet group, this pattern likely reflects a complex adjustment of oxidative homeostasis under nutrient imbalance. Similarly, cytochrome b5 reductase was significantly upregulated, consistent with the high saturated fatty acid content of the diet.

Comparable transcriptional adaptations to host-derived stress have been reported in other parasitic helminths. The liver fluke *Opisthorchis viverrine* showed in diabetic hamsters an upregulation of oxidative stress responses, immune evasion factors, and surface remodeling enzymes relative to healthy controls⁴². Likewise, *Echinococcus multilocularis* larvae downregulated growth-related genes while activating survival pathways for cellular maintenance and damage repair, facilitating long-term

persistence³⁹. These convergent patterns highlight the capacity of cestodes and trematodes to modulate transcriptional programs in response to nutritional and metabolic stressors.

In our study, gene expression analysis was performed only in Experiment 1, where worms experienced constant dietary stress from colonization onward. By contrast, the reversible suppression of reproduction in Experiment 2 occurred in adults that matured under fiber-rich conditions before short-term exposure to a Western diet. While the underlying transcriptional mechanisms remain unknown, the full restoration of egg production after diet reveal a distinct, reversible regulatory strategy. A comparable phenomenon occurs in *C. elegans*, where nutritional stress induces a quiescent state in adults without compromising developmental integrity³⁵. This raises the possibility that short-term reproductive arrest in *H. diminuta* reflects active stress-responsive signaling rather than developmental failure, warranting further investigation.

Because *H. diminuta* primarily inhabits the small intestine, our study focused on microbial communities in this specific niche. Dietary fiber emerged as a dominant driver of microbial community structure, consistent with recent *in vivo* evidence of strong diet-driven variation along the human small intestine⁴³. A fiber-rich diet enriched taxa linked to gut homeostasis, immune regulation, and host metabolism—such as Lactobacillales, *Turicibacter*, and Erysipelotrichales—mirroring previous fecal-based observations^{44–46}. These shifts are consistent with mechanistic evidence that fermentable fibers enhance SCFA production, strengthen epithelial barrier, and promote anti-inflammatory signaling⁴⁴.

In contrast, the Western diet generated a microbiota profile resembling those reported in human and animal models of fiber deprivation^{47–49}. This included a reduced abundance of fermentative taxa and an expansion of opportunistic and pro-inflammatory groups such as *Clostridia* and *Streptococcus*^{50,51}. Fiber deprivation is known to reduce SCFA-producing bacteria, favor mucin-degrading taxa, erode the mucus barrier, and increase epithelial exposure to pro-inflammatory signals⁴⁹. The lower alpha diversity observed in the Western diet group is a hallmark of diet-induced dysbiosis^{14,52,53}. The unchanged Simpson diversity index suggests the persistence of dominant taxa with the loss of less abundant, potentially beneficial species, narrowing ecological diversity. Beta diversity analyses further demonstrated that fiber deprivation produced compositionally unstable microbiotas, consistent with the ecological resilience conferred by dietary fiber^{44,54}.

Helminth colonization effects were strongly diet dependent. Under the fiber-rich diet, colonization induced only modest shifts, whereas under the Western diet it produced pronounced compositional changes, indicating that dysbiotic microbiotas are more susceptible to perturbation. Similar

diet-conditioned interactions have been reported for *T. suis* and *T. muris*, where microbial responses to helminths depend strongly on dietary background and fiber type^{15,16}.

Our metabolomic analysis confirms that diet composition is a key determinant of the small-intestinal chemical environment, aligning with *in vivo* evidence showing strong diet-driven variation in both dietary and microbially transformed metabolites^{43,54}. In our study, fructose—the main carbohydrate in the Western diet—was detected only in this group, reflecting its slower absorption compared with glucose⁵⁵ and reduced fermentation under fiber deprivation. This pattern was reinforced by the Western-diet microbiota, which contained fewer fermentative taxa (*Lactobacillales*, *Turicibacter*, *Erysipelotrichales*) and more opportunists (*Clostridia*, *Streptococcus*, *Staphylococcus*, *Burkholderiales*)^{47,48}. This shift reduces fructose utilization for short-chain fatty acid production and contributes to changes such as elevated conjugated bile acids linked to inflammation⁴⁸. While these observations highlight fructose as a potential driver of *H. diminuta* developmental arrest, its specific role requires targeted experimental testing.

By contrast, the fiber-rich diet maintained a chemically diverse lumen enriched in plant-derived and microbially transformed metabolites, reflecting its higher fermentation capacity^{43,47}. Under these conditions, *H. diminuta* colonization was associated with enrichment of diacylglycerols and amino acids absent in non-colonized rats, likely generated by helminth-induced microbial shifts or its metabolism. Limited glucose availability in the Western diet, together with the predominance of less favorable sugars such as sucrose and maltose⁵⁶, may contribute to the developmental arrest or aestivation-like state described above. Similar suppression of *H. diminuta* growth and reproduction has been reported under sucrose-based or carbohydrate-free diets⁵⁷, consistent with impaired reproductive maturation in the absence of appropriate nutritional cues. Fiber fermentation in the Accessible Fiber diet likely provides sufficient glucose to support normal parasite development.

The splenic cytokine gene-expression profile observed in *H. diminuta*-colonized rats fed the Accessible Fiber diet, marked by increased *Il4* and *Il13* expression, is consistent with a Th2-type anti-inflammatory response that is well established as a mechanism of helminth-induced immune modulation promoting host tolerance and tissue repair^{9,58}. This Th2-associated signal was not induced by colonization under the Western diet, where colonized rats instead showed elevated *Ifng* expression, suggesting that fiber deprivation alters the host–helminth–immune relationship, potentially through shifts in microbial composition^{44,49}. Consistent with this interpretation, *Il1b* expression was reduced in colonized rats on the fiber-rich diet. Together, these findings indicate that dietary fiber availability shapes whether *H. diminuta*

colonization is associated with a Th2-skewed, tolerogenic signature accompanied by reduced pro-inflammatory markers, or with a more pro-inflammatory profile under fiber-poor conditions. Under fiber-poor conditions, this immunomodulatory phenotype is diminished or redirected toward a more pro-inflammatory profile. Findings from other helminth models support this diet-dependent pattern. In *T. suis*, long-chain inulin enhances Th2 immunity, strengthens epithelial barrier function, and shifts the microbiota toward an anti-inflammatory profile¹⁵. In *T. muris*, however, the same fiber suppresses Th2 responses and promotes Th1 activity¹⁶. These contrasts show that immune outcomes depend not only on fiber availability but also on its type, fermentability, and the broader host–parasite–microbiome context.

Beyond immune modulation, our data indicate that the impact of *H. diminuta* colonization on host body weight is also strongly diet dependent. While most previous studies describe a protective effect of helminths against diet-induced weight gain^{59,60}, we observed the opposite pattern in Western diet–fed rats, where helminths amplified weight gain. This contrast suggests that the dysbiotic microbiota and metabolic profile characteristic of the Western diet may shift host–parasite interactions toward increased energy harvest. Potential mechanisms include enhanced intestinal absorption, altered gut transit time, and microbiota-mediated modulation of energy metabolism.

Our study demonstrates that dietary fiber content shapes the small intestinal microbiota, metabolome, and life-history strategies of the intestinal helminth *H. diminuta*. A fiber-rich diet supported a microbiota associated with gut homeostasis, a chemically diverse intestinal lumen, and full parasite growth and reproduction. In contrast, a Western-style, low-fiber diet created a dysbiotic, low-fermentation environment characterized by fructose accumulation and limited glucose availability, eliciting two stage-specific helminth responses: arrested development when deprivation occurred at colonization, and a reversible, aestivation-like suppression of reproduction in adult worms.

Transcriptomic profiling of developmentally arrested worms revealed coordinated downregulation of reproduction-, muscle-, and energy-related pathways alongside activation of oxidative stress responses, providing the first evidence of diet-driven transcriptional remodeling in a cestode. This plasticity likely facilitates persistence during nutritionally unfavorable conditions and illustrates how diet can directly regulate helminth physiology.

By shaping both microbial and chemical gut environments, diet indirectly influences helminth immune modulation and persistence. Given that *H. diminuta* can induce Th2-biased, anti-inflammatory responses via microbiota shifts, aligning dietary context may enhance the efficacy of helminth-based approaches for chronic inflammatory and autoimmune diseases.

Finally, diet-induced suppression of reproduction may mask helminth colonization when diagnostics rely solely on egg detection, suggesting that the prevalence of *H. diminuta* in humans and animal hosts may be underestimated under fiber-poor conditions. Long-term shifts toward low-fiber, high-fat diets may therefore contribute not only to helminth decline but also to adaptive changes in host–parasite–microbiome interactions. Future studies should dissect the causal roles of specific dietary components and metabolites, including fructose, in driving these responses.

ARTICLE IN PRESS

METHODS

Dietary setup

To test whether diet modulates the physiology and ecological function of *Hymenolepis diminuta* in the host gut, we examined how two contrasting dietary compositions affect its survival, development, and interaction with the intestinal environment. We intentionally selected two diets with markedly different nutritional profiles to uncover potential diet-driven changes in tapeworm condition and function.

The first diet was a Western-type diet rich in fat and processed sugar but devoid of microbe-accessible dietary fiber (TD.88137; Ssniff Spezialdiäten GmbH, Soest, Germany). It was composed primarily of casein (19.5%) as a protein source, and corn starch (15%), sucrose (33.4%) and butter fat (21%) as energy sources (although labelled as fiber-free, this diet contained 5% cellulose as a pellet-binding agent). The second diet was a standard laboratory rodent diet ST1 (feed mixture ST-1; Velas a.s., Lysá nad Labem, Czech Republic) with a high content of structurally diverse, microbe-accessible fiber and broader ingredient complexity. It consisted of 40% wheat, 22% soybean meal, 6% maize, 5% wheat bran, 3% oat rice, and 2.5% lucerne meal, with 10% fish meal as a protein source. Hereafter, we refer to this as the Accessible Fiber diet. For full composition and nutritional details of both diets see Table 1.

Animal housing and ethical approval

Outbred female Wistar rats (RccHan[®]: WIST; *Rattus norvegicus*), 13 weeks of age, were obtained for the experiment from Envigo RMS B.V. (Horst, Netherlands; the supplier Anlab s.r.o., Prague, Czech Republic). Sex was not considered as a biological variable in the study design and analysis. All rats were acclimated for seven days to the animal facility prior to the beginning of the experiment with *ad libitum* access to the standard laboratory chow and water. They were housed under controlled conditions in ventilated isolator cages with HEPA filters (Individually Ventilated machine SealSafe 1291H, Techniplast s.p.a., Buguggiate, Italy; the supplier: Trigon Plus a.s., Čestlice, Czech Republic) for the duration of the experiment, with continuous *ad libitum* access to the respective experimental diets and water. Their health status was visually inspected at 24-h intervals during daily routines, and they were euthanized by cervical dislocation (under anesthesia) at the end of the experiment. This study was approved by the Committee on the Ethics of Animal Experiments of the Biology Centre of the Czech Academy of Sciences (České Budějovice, Czechia, permit no. 33/2018) and by the Resort Committee of the Czech Academy of Sciences (Prague, Czech Republic) according in strict accordance with Czech legislation (Act No. 166/1999 Coll. on Veterinary Care and on Changes of Some Related Laws, and Act No. 246/1992 Coll. on the Protection of Animals against Cruelty), as well as the legislation of the European Union.

Culture of *Hymenolepis diminuta* and preparation of the inoculum

Under laboratory conditions, *H. diminuta* was maintained using grain beetles (*Tenebrio molitor*) as the intermediate host and outbred rats as the definitive host. Grain beetles were fed rat feces containing *H. diminuta* eggs to allow cysticercoids development. Cysticercoids were subsequently dissected directly from beetles harboring them. Each inoculum consisted of approximately ten cysticercoids, washed three times in sterile PBS (pH 7.4), and administered in a final volume of 100 μ l.

Experimental design

We conducted two experiments which were designed to assess how contrasting dietary compositions influence the viability, physiological condition, and ecological role of *H. diminuta* in the host gut. Each experiment included diet administration, colonization of rats with *H. diminuta*, and subsequent sample collection. In both experiments, rats were inoculated with a dose of cysticercoids using esophageal gavage. Successful colonization was confirmed by detecting eggs in the rats' feces using a modified Sheather's flotation method, conducted between 19- and 21-days post-inoculation²³.

Experiment 1: The aim of the first experiment was to determine how *H. diminuta* development responds to different host diets. Rats were maintained under defined dietary conditions for a total of 60 days and assigned to experimental groups based on diet and colonization status. The experimental timeline consisted of two phases (for details see Fig. 1A): (1) days 0–30, during which rats were fed either the Western diet or the Accessible Fiber diet prior to inoculation, and (2) days 30–60, when half of the rats were inoculated with *H. diminuta* and the remaining half received a placebo (PBS), while continuing on their respective diets. This period encompassed the prepatent period of tapeworm development to patent one (i.e. – development from larval to adult stage). All rats were euthanized on day 60 post-inoculation.

This experimental design resulted in four primary experimental groups (total $n = 88$): *H. diminuta*-colonized rats on the Western diet ($n = 48$), non-colonized rats on the Western diet ($n = 8$), *H. diminuta*-colonized rats on the Accessible Fiber diet ($n = 24$), and non-colonized rats on the Accessible Fiber diet ($n = 8$). Group sizes were determined based on a pilot experiment indicating arrested development of *H. diminuta* under the Western diet and an approximately 50% colonization success rate, necessitating increased rat numbers in the Western diet-colonized group.

Because *H. diminuta* is anatomically localized in the small intestine, intact recovery of tapeworms was incompatible with simultaneous collection of intestinal contents for microbiome and metabolomic

analyses. Colonized rats were therefore allocated to two analytical branches – a worm-centered branch comprising morphological and transcriptomic analyses ($n = 32$ Western diet; $n = 16$ Accessible Fiber diet), and a host-centered branch comprising gut microbiota profiling, metabolomic analyses of small intestinal contents, and cytokine gene expression analyses. The host-centered branch included colonized rats (Western diet $n = 16$; Accessible Fiber diet $n = 8$) and non-colonized controls from both diets (Western diet $n = 16$; Accessible Fiber diet $n = 8$). Under the Western diet, only rats with confirmed *H. diminuta* presence were included in host-centered analyses.

Experiment 2: This experiment examined whether diet-induced changes in adult tapeworm condition are reversible, using egg production as the primary outcome. The experimental design was informed by a pilot study assessing colonization success and egg output. The total number of rats ($n = 18$) were initially maintained on the Accessible Fiber diet for 30 days, then colonized with *H. diminuta* and kept on the same diet for an additional 20 days, covering the prepatent period. After this period, the rats were divided into three groups ($n = 6$ per group) according to dietary transitions (see Fig. 1B for details). The first control group continued the Accessible Fiber diet for the remainder of the experiment. The second control group was transitioned from the Accessible Fiber diet to the Western diet (day 50). The last group (experimental recovery group) underwent two dietary changes, initially switching from the Accessible Fiber diet to the Western diet (day 50), then returning to the Accessible Fiber diet after egg production ceased (day 60). The presence of *H. diminuta* eggs in the fecal samples (eggs per gram of feces) was monitored and quantified at two-day intervals and between days 50 and 60 every day. The number of eggs was counted using a McMaster chamber and Sheather's sugar solution.

Egg count data were preprocessed into long format (one row per animal per day) and annotated with experimental group (diet) and replicate (individual). Statistical analyses proceeded in three steps. First, daily group differences were tested using generalized linear models with a negative binomial distribution to account for overdispersion in count data; significant effects were followed by pairwise post hoc comparisons with false discovery rate (FDR) correction. Second, within-group temporal variation was evaluated by partitioning time into three biologically relevant intervals (<50, 50–59, ≥ 60 days, corresponding to dietary changes) and applying the same modeling framework to test for differences across intervals, followed by corrected post hoc contrasts. Third, to assess longitudinal dynamics, group-specific trajectories were modeled with time as a continuous predictor and interaction terms (group \times time) to test whether trends differed across diets. Where significant, group-level slopes and post hoc contrasts were estimated to quantify divergence.

In addition, day-by-day comparisons were performed within each diet group to identify significant temporal changes, and exploratory between-group comparisons were conducted to evaluate differences among dietary regimens. P-values were adjusted for multiple comparisons using the Bonferroni correction. Results were visualized using GraphPad Prism v10 software (San Diego, CA, USA).

Sampling & clinical assessment

In Experiment 1, on day 60, samples were collected downstream analyses. Consistent with experimental design, tapeworms were collected from successfully colonized rats for length measurements ($n = 16$ per group), as well as for morphological and transcriptomic analyses ($n = 8$ per group for each). Host-centered sampling included collection of spleen tissues for cytokine gene expression analysis ($n = 8$ per group), and small intestinal contents for bacteriome and metabolome analyses ($n = 8$ per group). For bacteriome and metabolome, fresh luminal contents of the small intestine (jejunum and ileum) were collected immediately after dissection, quickly homogenized by gentle mechanical mixing to obtain a uniform suspension, and divided into aliquots for downstream analyses.

Clinical parameters, particularly body weight, were collected in a blinded fashion²³ throughout the experiment at selected time points according to the experimental design ($n = 8$ per group; Fig. 1). Changes in body weight were expressed as percent change from day 0 (diet initiation). Longitudinal body-weight data were analyzed using three-way repeated-measures ANOVA with time as a within subject factor and diet, and colonization as between-subject factors, applying the Geisser–Greenhouse correction where appropriate. Post-hoc comparisons between treatment groups at individual time points were performed using Tukey's multiple comparisons test. Statistical analyses were conducted in R (R Core Team, 2013), and GraphPad Prism software v10 (San Diego, CA, USA) was used for data visualization.

Morphological analyses

Total of 32 *H. diminuta* specimens were measured, comprising one worm per rat from the Accessible Fiber diet group ($n = 16$) and one worm per rat from the Western diet group ($n = 16$). For statistical analysis, the rat was considered the experimental unit. Statistical significance was assessed using Welch's *t*-test.

For detailed morphological analyses, live tapeworms ($n = 8$ per group) were obtained during final necropsies on day 60 (Experiment 1). Because tapeworms from the Western diet were highly fragile, only six specimens were suitable for morphological analyses. Specimens were rinsed in saline, heat-killed in hot water (90 °C), and fixed in 4% formaldehyde solution. They were stained with Mayer's hydrochloric carmine, dehydrated through an ethanol series, cleared with eugenol, and mounted in Canada balsam on

slides. Moreover, pieces of strobila were embedded in paraffin wax, sectioned at 15 μm thickness, stained with hematoxylin–eosin, and mounted in Canada balsam. These specimens were examined and documented photographically using an Olympus BX51 microscope (Olympus Corp., Tokyo, Japan). The most representative tapeworms (11 specimens - three from the Western diet and eight from the Accessible Fiber diet) are deposited in the helminthological collection IPCAS-C200.

Differential gene expression and enrichment analyses

For transcriptomic analyses, a total of 16 *H. diminuta* specimens were used ($n = 8$ per group), Total RNA was isolated using the TRIzol reagent according to the manufacturer's protocol. Due to low RNA yield from undeveloped and very small *H. diminuta* individuals recovered from rats fed the Western diet, only three samples from this group met quality requirements for RNA library prep and led to satisfactory sequencing library construction. To maintain equal sample sizes between dietary groups, three specimens with the highest RNA quality were selected from the Accessible Fiber diet group.

Total RNA was isolated using the TRIzol reagent according to the manufacturer's protocol. RNA samples were prepared for Illumina sequencing using TruSeq Stranded mRNA Library Preparation Kit (Illumina, San Diego, CA, USA) and sequenced on a NextSeq 500 platform using High Output Kit v2.5 (150 cycles). RNA-seq reads for each sample were aligned to the *H. diminuta* genome (accession number GCA_902177915.1) using the STAR v2.7.3a aligner with the default parameters⁶¹. Reads with ambiguous assignment, multi-mapping, or overlapping features were excluded using SAMtools v1.11. The resulting alignments were used to quantify reads per gene using featureCounts of the subread v 2.0.1 R package⁶².

The expression matrix was uploaded to the online IDEP v0.96 platform⁶³, filtered using counts *per* million (CPM) with a cutoff of 0.5 in at least one library, and transformed using regularized log (rlog) transformation. The filtered dataset was used for exploratory data analysis (EDA), including principal component analyses (PCA) and k-means clustering. Gene clusters predicted by k means were subjected to functional enrichment analysis using ClusterProfiler v4.6.2 and the top 30 hits from topGo v 2.50.0 R packages.

Differentially expressed genes (DEGs) were detected using the DESeq2 v1.38.35 package⁶⁴. All genes with an adjusted p-value < 0.01 and an absolute fold-change ≥ 2 were subjected to enrichment analysis. Visualization and summary of significant DEGs were performed using the tidyverse v1.3.2, viridis v0.6.4, and pheatmap v1.0.12 R packages.

Analyses of small intestine bacteriome

Total DNA was purified using PSP® SPIN Stool DNA Plus Kit (Strattec Biomedical, Birkenfeld Germany) according to manufacturer protocol⁹. The microbiome analysis included samples from a total of 32 rats, divided into four experimental groups ($n = 8$ per group). PCR amplification was performed on the V3–V4 region of bacterial 16S rRNA with forward primer S-D-Bact-0341-b-S-17 (CCTACGGGNGGCWGCAG) and reverse S-D-Bact-0785-a-A-21 (GACTACHVGGGTATCTAATCC)⁶⁵. The high-throughput sequencing (HTS) library was generated using a two-step-PCR approach⁶⁶, employing Nextera primer design. Analyses were carried out in two technical replicates with different tag primer barcodes. Nuclease-free water and blank isolations were used as negative controls. The final library was sequenced using a MiSeq Reagent Kit v3 (2 × 300 bp pair-end reads, 600 cycles) on the Illumina MiSeq platform.

Gene-specific primers were trimmed using skewer v0.2.2 before using DADA2 v1.18 to assemble paired end reads, denoise the data set and eliminate low-quality reads (expected error rate >1)⁶⁷. To prevent artificial inflation of diversity caused by PCR/sequencing, only amplicon sequence variants (ASVs) consistently identified in both technical duplicates of each sample were included in the final dataset⁶⁶. To taxonomically assign ASVs, the naïve Bayesian RDP classifier (*assignTaxonomy*)⁶⁸ was implemented in the DADA2 pipeline. A training database of reference sequences was constructed using bacterial 16S sequences that were downloaded (February 2023) from the SILVA v138 database⁶⁹. To further filter the taxonomic dataset, all unclassified ASVs and those not assigned to Bacteria were manually removed.

All statistical analyses focused on variation in bacterial community composition between different types of diet (Accessible Fiber diet, Western diet) and colonization of *H. diminuta* (colonized, non-colonized). The bar charts, dot plots, and boxplots used to visualize the data were created in R Studio v0.99.489. First, variation of alpha diversity, by the number of different ASVs per sample (number of ASVs per sample = ASV richness) as a proxy measure was evaluated together with Simpson's diversity index (1-D). The effects of diet and colonization were tested using generalized linear models (GLMs) with quasipoisson error distribution (based on residual deviation) (stats R package; R Core Team, 2013). ANOSIM-based community compositional dissimilarities were used to investigate variation in beta diversity – differences in the bacterial diversity between diet and colonization groups – using Bray-Curtis Dissimilarities (accounting for relative abundances)⁷⁰ and the Jaccard index (only prevalence of ASVs is considered)⁷¹ assessed by permutation testing ($n = 999$), as implemented in the vegan R package. Clustering was visualized with PCoA (principal coordinates analysis) using the phyloseq R package⁷⁰. Last, linear discriminant analysis effect size method (LEfSe) were used for microbiome biomarker discovery between different types of diet⁷². To assess covariation between bacterial ASV relative abundance and relative metabolite abundance in samples of rats fed on different types of diet similarity measures

(Spearman's correlation for compositional data) were calculated through bootstrap and permutation matrices and by simple correlation test (stats R package).

Metabolomics

The metabolomics analysis included samples from a total of 32 rats, divided into four experimental groups ($n = 8$ per group). Each biological sample represents intestinal content collected from one individual rat. A pooled quality control (QC) sample was prepared by combining equal aliquots from all study samples. This pooled QC sample was injected at regular, equidistant intervals throughout the analytical batch, specifically after every seventh sample. Both positive and negative ionization modes (ESI+ and ESI-) were acquired within a single LC-MS analysis using polarity switching. Each biological sample was therefore measured once, without technical replicates. QC samples were processed and evaluated identically to the study samples and included in all downstream data processing steps. Repeated QC injections were used to monitor instrument stability and analytical reproducibility over the course of the batch. For each detected metabolite, variability observed across QC injections was used to estimate instrument-related (analytical) variance and to assess MS performance stability.

The deionized water was prepared using Direct Q 3UV (Merck, Prague, Czech Republic). LC/MS-grade (Optima™ LC/MS) methanol and acetonitrile were purchased from Fisher Scientific (Pardubice, Czech Republic), Ammonium carbonate and 4-Fluorophenylalanine (Sigma Aldrich, Prague, Czech Republic), 25% Ammonia solution (Merck, Prague, Czech Republic) and hexakis (2,2-difluoroethoxy) phosphazene and tris(trifluoromethyl)-1,3,5-triazene from Apollo Scientific (Bredbury, UK).

Samples of the small intestine content were dissected from the rats, weighed, and collected in 50 ml plastic Eppendorf vials. They were extracted using a cold extraction medium (MeOH:ACN (v/v) with 0.1% formic acid) at a 1:4 (w/w) ratio (intestine content/extraction medium). Exact sample weights are provided in Supplementary Data 2. This mixture was placed in an ultrasonic bath (10 min, 0°C), then the mixture was centrifuged (4650 g, 10 min, 4°C) and the supernatant was separated. 300 µL of the supernatant was removed for direct use, the remainder was stored at -80°C. 300 µL of the supernatant was filtered through a 0.2 µm PVDF mini-spin filter (HPST, Prague, Czech Republic) at 4650 g, 4°C, 5 min. 4-fluorophenylalanine (10 µL of 1 µg/µL) was used as a system suitability marker to verify analytical consistency across individual injections and added to the LC/MS injection vials and evaporated in a vacuum concentrator (RVC 2-25 CDplus, Martin Christ, Osterode am Harz, DE). 100 µL of the sample was then added to the vials containing the internal standard, mixed well, and measured with LC-HRMS. Extraction blanks and solvent blanks were prepared, injected, and processed alongside biological samples

to monitor background signals, potential contamination, and carryover throughout the analytical workflow.

The LC–MS methodology followed an established workflow and was implemented as described below and with reference to published protocols⁷³. An Orbitrap Q Exactive Plus combined with Dionex Ultimate 3000 and Dionex open autosampler (Thermo Fisher Scientific, San Jose, CA, USA) for the screening analysis were used. The Q Exactive mass spectrometer was operated in the ESI positive (PESI) and negative (NESI) ion mode (separate injection) for all detection. The instruments worked in Full MS scan mode; the mass range for positive mode was 75-1000 Da and it was 70-1000 Da for negative ion mode. The Q-Exactive settings were: 70,000 resolving power (scan rate at ± 3 Hz), 3×10^6 automatic gain control (AGC) target and maximum ion injection time (IT) 100 ms. Source ionization parameters were as follows: (+/-)3000 kV spray voltage, 350°C capillary temperature, sheath gas at 60 au, aux gas at 20 au, spare gas at 1 au, probe temperature 350°C and S-Lens level at 60 au. For accurate mass the lock mass 622.0290 Da (hexakis(2,2-difluoroethoxy)phosphazene) and 301.9981 Da (tris(trifluoromethyl)-1,3,5-triazene) were used for positive and negative ion mode, respectively. Chromatographic separation was carried out on the SeQuant ZIC-pHILIC (150mm x 4.6 mm i.d., 5 μ m, Merck KGaA, Darmstadt, Germany), the flow rate of 450 μ L/min, the injection volume of 5 μ L, column temperature of 35°C and mobile phase gradient: 0 min, 20% B; 20 min, 80% B; 20.1 min, 95% B; 23.3 min, 95% B; 23.4 min, 20% B; 30.0 min 20% B, where A was acetonitrile and B was 20 mmol/L aqueous ammonium carbonate (pH = 9.2; adjusted by NH₄OH). The data were acquired and processed using homemade software MetaboliteMapper and Xcalibur software v2.1 (Thermo Fisher Scientific, San Jose, CA, USA).

Metabolite annotation was performed using accurate mass matching (≤ 3 ppm mass error), chromatographic retention time alignment, and MS/MS spectral comparison against an in-house curated metabolite reference library implemented in MetaboliteMapper. Where authentic chemical standards were available, compound identities were confirmed based on matching retention time and MS/MS spectra (MSI level 1). For metabolites lacking reference standards, putative annotations were assigned based on accurate mass, retention time, and MS/MS spectral similarity (MSI level 2). In total, 397 metabolites were annotated, including 146 confirmed by authentic standards (MSI level 1), 227 supported by MS/MS spectral matching (MSI level 2), and 24 assigned based on accurate mass matching only (MSI level 3). (Detailed Metabolite annotation summary is available on Figshare DOI: XXX).

The data obtained from the metabolite's peak areas were statistically evaluated using ordination methods as follows: for all data – detrended correspondence analysis (DCA); for linear data – principal component analysis (PCA), redundancy analysis (RDA), and Monte-Carlo permutation test (unrestricted

permutations, $n=999$). The data was transformed using a particular sample's internal standard peak area, followed by logarithmic transformation. PCA analysis was used to visualize the data. In the canonical analysis (RDA), the diet and colonization were nominal ecological variables. In the canonical analysis (RDA), the diet and colonization were nominal ecological variables. Statistic software CANOCO 4.5 (Biometris, Plant Research International, Wageningen UR, Netherlands) was used for the DCA, PCA, RDA, and Monte-Carlo permutation test analyses.

Analyses of immune markers

To evaluate relative gene expression of immune markers, a portion of the spleen (approximately 150-250 mg) was collected from individual rats ($n = 8$ per group; in total 32 rats). Total RNA was isolated using the Hybrid-R™ kit (GeneAll Biotechnology, Seoul, Korea) and then reverse transcribed to cDNA using the High-Capacity RNA-to-cDNA kit (Thermo Fisher Scientific, Waltham, MA, USA). qPCR analyses were performed using commercially available TaqMan gene expression assays (Thermo Fisher Scientific) with rat-specific probes for *I11b* (amplicon length – 74 bp; Assay ID: Rn00580432), *Ifng* (amplicon length – 91 bp; Assay ID: Rn00594078), *I14* (amplicon length – 85 bp; Assay ID: Rn99999010), *I13* (amplicon length – 95 bp; Rn00587615) and *B2m* as housekeeping (amplicon length – 58 bp; Assay ID: Rn00560865). Each biological sample was analyzed in technical duplicates. qPCR reactions were run according to the manufacturer's protocols (Thermo Fisher Scientific) on a LightCycler 480 system (Roche, Basel, Switzerland). Relative cytokine gene expression was calculated using the Pfaffl method⁷⁴ and normalized to B2M using R software v.4.3.1. Group differences were analyzed using the Kruskal–Wallis test followed by Dunn's multiple comparisons test with adjustment for multiple testing. Data were visualized using GraphPad Prism Software v10 (San Diego, CA, USA)

Data Availability

Transcriptomic data generated in this study are deposited in the NCBI Sequence Read Archive under accession code [PRJNA1126432](https://www.ncbi.nlm.nih.gov/seqread/PRJNA1126432). Bacteriome sequencing data are archived in the European Nucleotide Archive under accession code [PRJEB86956](https://www.ebi.ac.uk/ena/record/PRJEB86956). Metabolomics data and additional source data supporting the findings of this study—including images and videos of *Hymenolepis diminuta*, worm length measurements, egg counts, cytokine relative and Cp values, raw and relative body weight data, a checklist of bacteriome sequences, and a table of metabolite annotations and standards are available in the Figshare repository under accession DOI: XXXX [<https://figshare.com/s/df77505840944a777748>]. Detailed methodological protocols are available from the corresponding author upon request.

REFERENCES:

1. Fan, Y. & Pedersen, O. Gut microbiota in human metabolic health and disease. *Nat Rev Microbiol* **19**, 55–71 (2021).
2. Garcia-Bonete, M. J., Rajan, A., Suriano, F. & Layunta, E. The underrated gut microbiota helminths, bacteriophages, fungi, and archaea. *Life* **13**, 1765 (2023).
3. Lukeš, J., Stensvold, C. R., Jirků-Pomajbíková, K. & Wegener Parfrey, L. Are human intestinal eukaryotes beneficial or commensals? *PLoS Pathog* **11**, e1005039 (2015).
4. Chibani, C. M. *et al.* A catalogue of 1,167 genomes from the human gut archaeome. *Nat Microbiol* **7**, 48–61 (2022).
5. Sobotková, K. *et al.* Helminth therapy – From the parasite perspective. *Trends Parasitol* **35**, 501–515 (2019).
6. Han, G. & Vaishnav, S. Microbial underdogs: exploring the significance of low-abundance commensals in host-microbe interactions. *Exp Mol Med* **55**, 2498–2507 (2023).
7. Rook, G., Bäckhed, F., Levin, B. R., McFall-Ngai, M. J. & McLean, A. R. Evolution, human-microbe interactions, and life history plasticity. *The Lancet* **390**, 521–530 (2017).
8. Reynolds, L. A., Finlay, B. B. & Maizels, R. M. Cohabitation in the intestine: Interactions among helminth parasites, bacterial microbiota, and host immunity. *J Immunol* **195**, 4059–4066 (2015).
9. Jirků, M. *et al.* Helminth interactions with bacteria in the host gut are essential for its immunomodulatory effect. *Microorganisms* **9**, 226 (2021).
10. Williams, A. R. *et al.* Emerging interactions between diet, gastrointestinal helminth infection, and the gut microbiota in livestock. *BMC Vet Res* **17**, 62 (2021).
11. Wammes, L. J. *et al.* Community deworming alleviates geohelminth-induced immune hyporesponsiveness. *Proc Natl Acad Sci USA* **113**, 12526–12531 (2016).
12. Weinstock J.V. The worm returns. *Nature* **491**, 183–185 (2012).
13. Venkatakrisnan, A. *et al.* Evolution of bacteria in the human gut in response to changing environments: An invisible player in the game of health. *Comput Struct Biotechnol J* **19**, 752–758 (2021).
14. You, C., Jirků, M., Corcoran, D. L., Parker, W. & Jirků-Pomajbíková, K. Altered gut ecosystems plus the microbiota's potential for rapid evolution: A recipe for inevitable change with unknown consequences. *Comput Struct Biotechnol J* **19**, 5969–5977 (2021).
15. Myhill, L. J. *et al.* Mucosal barrier and Th2 immune responses are enhanced by dietary inulin in pigs infected with *Trichuris suis*. *Front Immunol* **9**, 2557 (2018).
16. Myhill, L. J. *et al.* Fermentable dietary fiber promotes helminth infection and exacerbates host inflammatory responses. *J Immunol* **204**, 3042–3055 (2020).
17. Carvalho, N., Neves, J. H. das, Pennacchi, C. S. & Amarante, A. F. T. do. Hypobiosis and development of *Haemonchus contortus* and *Trichostrongylus colubriformis* infection in lambs under different levels of nutrition. *Ruminants* **3**, 401–412 (2023).
18. Daniel, H. Gut physiology meets microbiome science. *Gut Microbiome* **4**, 1–14 (2023).
19. Weiss, A. S. *et al.* Nutritional and host environments determine community ecology and keystone species in a synthetic gut bacterial community. *Nat Commun* **14**, 4780 (2023).
20. Loke, P. & Harris, N. L. Networking between helminths, microbes, and mammals. *Cell Host Microbe* **31**, 464–471 (2023).
21. Sulima-Celińska, A., Kalinowska, A. & Młocicki, D. The tapeworm *Hymenolepis diminuta* as an important model organism in the experimental parasitology of the 21st Century. *Pathogens* **11**, 1439 (2022).
22. Reyes, J. L. *et al.* Macrophages treated with antigen from the tapeworm *Hymenolepis diminuta* condition CD25⁺ T cells to suppress colitis. *FASEB J* **33**, 5676–5689 (2019).

23. Pomajbíková, K. J. *et al.* The benign helminth *Hymenolepis diminuta* ameliorates chemically induced colitis in a rat model system. *Parasitology* **145**, 1324–1335 (2018).
24. Williamson, L. L. *et al.* Got worms? Perinatal exposure to helminths prevents persistent immune sensitization and cognitive dysfunction induced by early-life infection. *Brain Behav Immun* **51**, 14–28 (2016).
25. McKenney, E. A. *et al.* Alteration of the rat cecal microbiome during colonization with the helminth *Hymenolepis diminuta*. *Gut Microbes* **6**, 182–193 (2015).
26. Parfrey, L. W. *et al.* A benign helminth alters the host immune system and the gut microbiota in a rat model system. *PLoS One* **12**, e0182205 (2017).
27. Shute, A. *et al.* Worm expulsion is independent of alterations in composition of the colonic bacteria that occur during experimental *Hymenolepis diminuta*-infection in mice. *Gut Microbes* **11**, 497–510 (2020).
28. Cheng, A. M., Jaint, D., Thomas, S., Wilson, J. K. & Parker, W. Overcoming evolutionary mismatch by self-treatment with helminths: Current practices and experience. *J Evol Med* **3**, 235910 (2015).
29. Liu, J., Morey, R. A., Wilson, J. K. & Parker, W. Practices and outcomes of self-treatment with helminths based on physicians' observations. *J Helminthol* **91**, 267–277 (2017).
30. Mettrick, D. F. The intestine as an environment for *Hymenolepis diminuta*. In *Biology of the tapeworm Hymenolepis diminuta* (ed. Arai, H. P.) 281–356 (Academic Press Inc., New York, 1980).
31. Jiang, C., Storey, K. B., Yang, H. & Sun, L. Aestivation in nature: Physiological strategies and evolutionary adaptations in hypometabolic states. *Int J Mol Sci* **24**, 14093 (2023).
32. Hand, S. C., Denlinger, D. L., Podrabsky, J. E. & Roy, R. Mechanisms of animal diapause: recent developments from nematodes, crustaceans, insects, and fish. *J Physiol Regul Integr Comp Physiol* **310**, 172 (2016).
33. Diniz, D. F. A., De Albuquerque, C. M. R., Oliva, L. O., De Melo-Santos, M. A. V. & Ayres, C. F. J. Diapause and quiescence: Dormancy mechanisms that contribute to the geographical expansion of mosquitoes and their evolutionary success. *Parasit Vectors* **10**, 310 (2017).
34. Yang, Q. *et al.* Transcriptome and metabolome analyses of sea cucumbers *Apostichopus japonicus* in Southern China during the summer aestivation period. *J Ocean Univ China* **20**, 198–212 (2021).
35. Makino, M., Ulzii, E., Shirasaki, R., Kim, J. & You, Y. J. Regulation of satiety quiescence by neuropeptide signaling in *Caenorhabditis elegans*. *Front Neurosci* **15**, 678590 (2021).
36. Schmeisser, K. *et al.* Mobilization of cholesterol induces the transition from quiescence to growth in *Caenorhabditis elegans* through steroid hormone and mTOR signaling. *Commun Biol* **7**, 121 (2024).
37. Komuniecki, R. & Roberts, L. S. Developmental physiology of cestodes. XIV. Roughage and carbohydrate content of host diet for optimal growth and development of *Hymenolepis diminuta*. *J Parasitol* **61**, 427–433 (1975).
38. Mettrick, D. F. Competition for ingested nutrients between the tapeworm *Hymenolepis diminuta* and the rat host. *Can J Public Health* **64**, 70–82 (1973).
39. Herz, M. *et al.* Genome-wide transcriptome analysis of *Echinococcus multilocularis* larvae and germinative cell cultures reveals genes involved in parasite stem cell function. *Front Cell Infect Microbiol* **14**, 1335946 (2024).
40. Patel, B. *et al.* Voltage gated proton channels modulate mitochondrial reactive oxygen species production by complex I in renal medullary thick ascending limb. *Redox Biol* **27**, 101191 (2019).
41. Kawai, T. *et al.* Regulation of hepatic oxidative stress by voltage-gated proton channels (Hv1/VSOP) in Kupffer cells and its potential relationship with glucose metabolism. *FASEB J* **34**, 15805–15821 (2020).

42. Chaidee, A. et al. Transcriptome changes of liver fluke *Opisthorchis viverrini* in diabetic hamsters. *Parasite* **31**, 54 (2024).
43. Folz, J. et al. Human metabolome variation along the upper intestinal tract. *Nat Metab* **5**, 777–788 (2023).
44. Makki, K., Deehan, E. C., Walter, J. & Bäckhed, F. The impact of dietary fiber on gut microbiota in host health and disease. *Cell Host Microbe* **23**, 705–715 (2018).
45. Kaakoush, N. O. Insights into the role of Erysipelotrichaceae in the human host. *Front Cell Infect Microbiol* **5**, 84 (2015).
46. Lynch, J. B. et al. Gut microbiota *Turicibacter* strains differentially modify bile acids and host lipids. *Nat Commun* **14**, 3669 (2023).
47. Beisner, J., Gonzalez-Granda, A., Basrai, M., Damms-Machado, A. & Bischoff, S. C. Fructose-induced intestinal microbiota shift following two types of short-term high-fructose dietary phases. *Nutrients* **12**, 3444 (2020).
48. Montrose, D. C. et al. Dietary fructose alters the composition, localization, and metabolism of gut microbiota in association with worsening colitis. *Cell Mol Gastroenterol Hepatol* **11**, 525–550 (2021).
49. Desai, M. S. et al. A dietary fiber-deprived gut microbiota degrades the colonic mucus barrier and enhances pathogen susceptibility. *Cell* **167**, 1339–1353 (2016).
50. Lloyd-Price, J. et al. Multi-omics of the gut microbial ecosystem in inflammatory bowel diseases. *Nature* **569**, 655–662 (2019).
51. Cani, P. D. Human gut microbiome: Hopes, threats and promises. *Gut* **67**, 1716–1725 (2018).
52. Louis, P., Solvang, M., Duncan, S. H., Walker, A. W. & Mukhopadhyay, I. Dietary fibre complexity and its influence on functional groups of the human gut microbiota. *Proc Nutr Soc* **80**, 386–397 (2021).
53. Morrison, K. E., Jašarević, E., Howard, C. D. & Bale, T. L. It's the fiber, not the fat: Significant effects of dietary challenge on the gut microbiome. *Microbiome* **8**, 15 (2020).
54. Meyer, R. K., Bime, M. A. & Duca, F. A. Small intestinal metabolomics analysis reveals differentially regulated metabolite profiles in obese rats and with prebiotic supplementation. *Metabolomics* **18**, 60 (2022).
55. Davidson, R. E., Leese, H. J. & Davidson, R. E. Sucrose absorption by the rat small intestine *in vivo* and *in vitro*. *J Physiol* **267**, 237–248 (1977).
56. Dunkley, L. C., Metrick, D. F. & Dunkley, L. C. A. *Hymenolepis diminuta*: Effect of quality of host dietary carbohydrate on growth. *Exp Parasitol* **25**, 146–161 (1969).
57. Roberts, L. S. & Platzer, E. G. Developmental physiology of cestodes. II. Effects of changes in host dietary carbohydrate and roughage on previously established *Hymenolepis diminuta*. *J Parasitol* **53**, 85–93 (1967).
58. Vacca, F. & Le Gros, G. Tissue-specific immunity in helminth infections. *Mucosal Immunol* **15**, 1212–1223 (2022).
59. Queiroz-Glauss, C. P. et al. Helminth infection modulates number and function of adipose tissue Tregs in high fat diet-induced obesity. *PLoS Negl Trop Dis* **16**, e0010105 (2022).
60. Su, C. wen et al. Helminth infection protects against high fat diet-induced obesity via induction of alternatively activated macrophages. *Sci Rep* **8**, 4607 (2018).
61. Dobin, A. et al. STAR: Ultrafast universal RNA-seq aligner. *Bioinformatics* **29**, 15–21 (2013).
62. Liao, Y., Smyth, G. K. & Shi, W. FeatureCounts: An efficient general-purpose program for assigning sequence reads to genomic features. *Bioinformatics* **30**, 923–930 (2014).
63. Ge, S. X., Son, E. W. & Yao, R. iDEP: An integrated web application for differential expression and pathway analysis of RNA-Seq data. *BMC Bioinformatics* **19**, 534 (2018).

64. Love, M. I., Huber, W. & Anders, S. Moderated estimation of fold change and dispersion for RNA-seq data with DESeq2. *Genome Biol* **15**, 550 (2014).
65. Klindworth, A. et al. Evaluation of general 16S ribosomal RNA gene PCR primers for classical and next-generation sequencing-based diversity studies. *Nucleic Acids Res* **41**, e1 (2013).
66. Pafčo, B. et al. Metabarcoding analysis of strongylid nematode diversity in two sympatric primate species. *Sci Rep* **8**, 5933 (2018).
67. Callahan, B. J. et al. DADA2: High-resolution sample inference from Illumina amplicon data. *Nat Methods* **13**, 581–583 (2016).
68. Wang, Q., Garrity, G. M., Tiedje, J. M. & Cole, J. R. Naïve Bayesian classifier for rapid assignment of rRNA sequences into the new bacterial taxonomy. *Appl Environ Microbiol* **73**, 5261–5267 (2007).
69. Quast, C. et al. The SILVA ribosomal RNA gene database project: Improved data processing and web-based tools. *Nucleic Acids Res* **41**, 5261–5267 (2013).
70. McMurdie, P. J. & Holmes, S. Waste not, want not: Why rarefying microbiome data is inadmissible. *PLoS Comput Biol* **10**, e1003531 (2014).
71. Hancock, J. M. Jaccard distance (Jaccard Index, Jaccard Similarity Coefficient). In: Dictionary of bioinformatics and computational biology (eds. Grant, P. & Mandal, S. S.) (John Wiley & Sons, 2004).
72. Segata, N. et al. Metagenomic biomarker discovery and explanation. *Genome Biol* **12**, 860 (2011).
73. Moos, M. et al. Cryoprotective metabolites are sourced from both external diet and internal macromolecular reserves during metabolic reprogramming for freeze tolerance in drosophilid fly, *Chymomyza costata*. *Metabolites* **12**, 163 (2022).
74. Pfaffl MW. A new mathematical model for relative quantification in real-time RT-PCR. *Nucleic Acid Res* **29**, e45.

ACKNOWLEDGEMENTS

This work was financially supported by the Ministry of Education, Youth and Sports of the Czech Republic under the INTER-EXCELLENCE programme (grant no. LTAUSA19008 to K.J.), by the Research Council of Norway (grant no. 324516 to K.J. and M.K.), by the ERD fund project Centre for Research of Pathogenicity and Virulence of Parasites (project no. CZ.02.1.01/0.0/0.0/16_019/0000759 to M.K., M.O., J.L.), and by the Czech Science Foundation (grant no. 23-07990S to R.K. and 25-15298S to J.L.). We acknowledge the CF Genomics CEITEC MU, provided through the NCMG research infrastructure (LM2023067 funded by MEYS CR), for their support with obtaining scientific data presented in this paper. Computational resources were provided by the e-INFRA CZ project (ID: 90254), supported by the Ministry of Education, Youth and Sports of the Czech Republic. We are grateful to the anonymous reviewers for their insightful comments and guidance during the review process.

AUTHOR CONTRIBUTION STATEMENT

M.J. conceptualized the study, developed methodology, conducted software analyses, performed investigation, carried out formal analysis and data curation, contributed to writing, produced visualizations, validated results, and supervised the work.

W.P. contributed to conceptualization and methodology, performed software analyses and investigation, carried out formal analysis and data curation, contributed to writing, produced visualizations, validated results, and supervised the work.

O.K. contributed to methodology, software, investigation, visualization, validation, and supervision.

M.K. contributed to conceptualization, methodology, software, investigation, formal analysis, and data curation, contributed to writing, produced visualizations, validated results, and supervised the work.

V.I. contributed to methodology, software, investigation, visualization, validation, and supervision.

M.M.W. contributed to conceptualization, methodology, software, investigation, data curation, writing, visualization, validation, and supervision.

R.K. contributed to methodology, software, investigation, visualization, validation, and supervision.

M.Mo. contributed to methodology, software, investigation, visualization, validation, and supervision.

P.T. contributed to methodology, software, investigation, visualization, validation, and supervision.

A.T. contributed to methodology, software, investigation, visualization, validation, and supervision.

Z.P. contributed to methodology, software, investigation, visualization, validation, and supervision.

K.B. contributed to methodology, software, investigation, visualization, validation, and supervision.

J.L. performed formal analysis and contributed to writing.

M.O. contributed to conceptualization, software, formal analysis, data curation, writing, visualization, validation, and supervision.

B.P. contributed to conceptualization, methodology, software, investigation, data curation, writing, visualization, validation, and supervision.

K.J. conceptualized the study, developed methodology, performed software analyses and investigation, carried out formal analysis and data curation, contributed to writing, produced visualizations, validated results, and supervised the work.

COMPETING INTERESTS

Coauthor W.P. has licensed intellectual property related to helminth therapy, which is owned by Duke University. This intellectual property is unrelated to the experimental design, data generation, analysis, or interpretation of the results presented in this study. The remaining authors declare that they have no competing interests.

ARTICLE IN PRESS

TABLE 1: Composition of experimental diets. Main ingredients and proximate composition of the Accessible Fiber diet (ST-1; Altromin, Czech Republic) and the Western diet (TD.88137; Ssniff, Germany). Detailed composition, including full amino acid and fatty acid profiles, vitamins, minerals, and additives, is available from the manufacturers. Values are expressed as mass percentage of diet (% w/w) or per kg diet, as indicated.

COMPONENTS	ACCESSIBLE FIBER DIET	WESTERN DIET
Main ingredients (% w/w)	wheat (40); soybean meal (22); fish meal (10); maize (6); wheat bran (5); oat rice (3); lucerne meal (2.5); feed yeast (2.5); dried milk (1.5); sugar (trace); Ca carbonate, Ca dihydrogen phosphate	sucrose (33.4); butter fat (21); casein (19.5); corn starch (15); cellulose powder (5); cholesterol (0.21);
Proximate composition (% of diet)	protein (24); fat (3.4); crude fiber (4.6.8)	protein (17.3); fat (21.1); crude fiber (5.0); ash (4.2); starch (14.4); sugar (3.3);
Selected amino acids (% of diet)	Lys (1.40); Met (0.48)	Lys (1.43); Met (0.93); Thr (0.76); Trp (0.22); Leu (1.71); Val (0.95)
Vitamins (per kg diet)	Vit A (28,000 IU); Vit D (2,200 IU); Vit mg)	Vit A (15,000 IU); Vit D3 (1,500 IU); Vit E (200 mg); Ascorbic Acid (0.1 mg); Choline Chloride (920 mg); Butylated hydroxytoluene (0.01 %);
Trace elements (per kg diet)	Cu (20 mg); Se (0.38 mg); Na (as NaCl, supplemented)	Fe (49 mg); Zn (29 mg); Cu (11 mg); Mn (95 mg); I (0.3 mg); Se (0.2 mg);

LEGENDS TO FIGURES:

Fig. 1 | Experimental design of dietary and *Hymenolepis diminuta* colonization studies.

A, Schematic overview of Experiment 1 showing acclimation, dietary allocation, inoculation with *H. diminuta* on day 30, experimental group formation, and sampling throughout the experiment (red squares – clinical data collection) and terminal sampling at day 60 (black squares – spleen samples; black circle – gut content samples; black triangle – worm samples). Rats were maintained on either an Accessible Fiber diet (AD, blue) or a Western diet (WD, pink) and were either colonized (C) or non-colonized controls (NC). Experiment 1 included four primary groups (total $n = 88$): colonized rats on the Western diet ($n = 48$), non-colonized rats on the Western diet ($n = 8$), colonized rats on the Accessible Fiber diet ($n = 24$), and non-colonized rats on the Accessible Fiber diet ($n = 8$). Because intact recovery of tapeworms was incompatible with simultaneous collection of intestinal contents, colonized rats were allocated either to worm-centered analyses (morphology and transcriptomics) or host-centered analyses (microbiota, metabolomics, and cytokine gene expression; final $n = 8$ per diet). Non-colonized controls ($n = 8$ per diet) were included in host-centered analyses. Under the Western diet, only rats with confirmed *H. diminuta* presence were included. **B**, Schematic overview of Experiment 2 illustrating *H. diminuta* inoculation, dietary switches between the Accessible Fiber and Western diets, and longitudinal egg count sampling. All rats were initially maintained on the Accessible Fiber diet; selected groups were switched to the Western diet and subsequently returned to the fiber-rich diet ($n = 6$ per group). Egg counts were collected every two days outside the patent period and daily during the patent period. Abbreviations: AD, Accessible Fiber diet; WD, Western diet; C, colonized rats; NC, non-colonized rats. (figure was created by the authors using Canva Pro license).

Fig. 2 | Morphological differences in *Hymenolepis diminuta* under distinct dietary conditions.

A, C and E, Representative adult *H. diminuta* recovered from rats fed the Accessible Fiber diet ($n = 8$). **B and D**, Developmentally arrested tapeworms recovered from rats maintained on the Western diet ($n = 6$). **A and B**, Whole-worm morphology. **C**, Mature proglottids. **D**, Immature proglottids. **E**, Gravid proglottids. Images shown in panels C–E are representative of observations obtained from one experiment, based on tapeworms recovered from at least six independent rats per group, with consistent morphology observed across rats. **F**, Comparison of *H. diminuta* length between dietary groups. Tapeworms recovered from rats fed the Accessible Fiber diet were significantly longer than those recovered from rats fed the Western diet (Western diet: 2.69 ± 1.41 cm, $n = 16$; Accessible Fiber diet: 20.81 ± 2.74 cm, $n = 16$; mean difference = 18.13 ± 0.77 cm; 95% confidence interval 16.53–19.72; Welch's two-sided t -test, $t(22.43) = 23.49$, $p < 0.0001$; $\eta^2 = 0.96$). Data are presented as mean \pm SD; each data point represents one biological replicate (one rat). Anatomical structures are indicated as follows: c, cirrus sac; e, egg; o, ovary; s, seminal vesicle; t, testes; u, uterus.

Fig. 3 | Diet-driven reversibility of egg production in *Hymenolepis diminuta*.

Egg counts (eggs/g feces) were measured longitudinally in colonized rats maintained on a continuous Accessible Fiber diet (blue; $n = 6$), switched to a Western diet (pink; $n = 6$), or switched to a Western diet and subsequently returned to the Accessible Fiber diet (black; $n = 6$). Monitoring began at the onset of patency (day 21). Transition to the Western diet on day 50 caused a rapid decline in egg output, resulting in cessation of egg shedding, whereas reintroduction of the fiber-rich diet restored reproductive activity. Longitudinal differences among dietary groups were assessed using negative binomial generalized linear models with a group \times time interaction,

followed by post hoc contrasts with FDR correction. A significant interaction was observed using two-sided testing ($\chi^2(2) = 290.8, p < 2.2 \times 10^{-16}$), indicating divergent temporal trajectories of egg production across diets. Colored brackets denote significant within-group differences across dietary phases; black asterisks indicate significant between-group differences at individual time points based on two-sided post hoc contrasts with FDR correction. Egg counts are presented as mean \pm SEM; error bars are shown for visualization purposes only. Each data point represents a biological replicate (individual rat), with repeated longitudinal measurements obtained from the same individual over time. Statistical significance is indicated as: ns (non-significant), $*p = 0.05$ – 0.01 , $**p = 0.01$ – 0.001 , $***p < 0.001$.

Fig. 4 | Diet-dependent gene expression patterns and functional enrichment in *Hymenolepis diminuta*.

A, Normalized expression profiles of differentially expressed genes across individual biological samples of *H. diminuta* recovered from rats fed the Western diet (WD1–WD3) and the Accessible Fiber diet (AD1–AD3) ($n = 3$ biological replicates per diet). The x-axis denotes individual samples, and the y-axis shows normalized gene expression values. Thin gray lines represent individual genes, whereas colored lines (green for Western Diet and orange for Accessible Fiber diet) indicate the mean expression profile across all differentially expressed genes within each dietary condition. Numbers indicate the total number of genes contributing to each enriched category for genes downregulated or upregulated under the Western diet. Each biological replicate corresponds to tapeworms recovered from an individual rat. B, Gene Ontology (GO) functional enrichment analysis of differentially expressed genes identified between dietary conditions (FDR < 0.01 , $|\log_2FC| > 1$). GO enrichment was performed using topGO, and significantly enriched GO terms are grouped into Biological Process, Cellular Component, and Molecular Function categories.

Fig. 5 | Differential enrichment of bacterial taxa in the small intestine in relation to diet and *Hymenolepis diminuta* colonization.

A, Linear discriminant analysis (LDA) scores of bacterial taxa differentially enriched between rats fed an Accessible Fiber diet (blue) and a Western diet (pink). B, LDA scores of bacterial taxa differentially enriched between non-colonized and colonized rats under the Accessible Fiber diet; no taxa were identified as significantly enriched in colonized rats under this dietary condition. C, LDA scores of bacterial taxa differentially enriched between colonized (light pink) and non-colonized (dark pink) rats under the Western diet. For all panels, enrichment analysis was performed using LEfSe (Linear discriminant analysis Effect Size). LDA scores $|\log_{10}|$ indicate the effect size associated with each differentially enriched taxon, which are listed along the y-axis. Only taxa with LDA scores above the significance threshold are shown. Each group consisted of $n = 8$ biological replicates *per* group (individual rat).

Fig. 6 | Impact of diet and *Hymenolepis diminuta* colonization on small intestinal bacterial diversity.

A and B, Boxplots showing alpha diversity metrics of the small intestinal bacteriome, including amplicon sequence variant (ASV) richness (A) and Simpson's diversity index (B), for colonized and non-colonized rats maintained on an Accessible Fiber diet (A-diet, blue) or a Western diet (W-diet, pink; $n = 8$ *per* group). The center line denotes the mean, boxes represent the interquartile range (25th–75th percentiles), whiskers extend to the minimum and maximum values, and black dots indicate individual samples. Differences in alpha diversity were assessed using generalized

linear models, revealing significantly lower diversity under the Western diet compared to the Accessible Fiber diet (ASV richness, $p < 0.001$; Simpson's index, $p < 0.01$), independent of colonization status. **C and D**, Principal coordinates analysis (PCoA) plots depicting beta diversity based on Bray–Curtis dissimilarities (C) and the Jaccard index (D). Each data point represents one biological replicate (individual rat), with symbols indicating colonized (circles) and non-colonized (triangles) animals. Ellipses represent 95% confidence intervals, and axes indicate the percentage of variance explained. Differences in community composition between dietary groups were assessed using analysis of similarities (ANOSIM), revealing strong diet-driven separation (Bray–Curtis: $R = 0.8683$, $p = 0.001$; Jaccard: $R = 0.781$, $p = 0.001$).

Fig. 7 | Beta diversity of the small intestinal bacteriome in response to *Hymenolepis diminuta* colonization.

A and B, Principal coordinates analysis (PCoA) plots showing bacterial community profiles in rats fed an Accessible Fiber diet, based on Bray–Curtis dissimilarities (A) and the Jaccard index (B). Each point represents an individual sample ($n = 8$ per group), with colonized rats shown as light blue circles and non-colonized rats as dark blue triangles. **C and D**, PCoA plots showing bacterial community profiles in rats fed a Western diet, based on Bray–Curtis dissimilarities (C) and the Jaccard index (D). Each point represents an individual sample ($n = 8$ per group), with colonized rats shown as pink circles and non-colonized rats as red triangles. Each point represents one biological replicate (individual rat). Ellipses represent 95% confidence intervals for each group, and axes indicate the percentage of variance explained.

Fig. 8 | Diet- and colonization-dependent effects on the small intestinal metabolome.

A, Principal component analysis (PCA) showing clustering of small intestinal metabolomic profiles according to diet and *Hymenolepis diminuta* colonization status. Each point represents an individual sample ($n = 8$ per group). Samples are grouped by Western diet colonized (W-HD, pink circles with outline), Western diet non-colonized (W-NC, light pink circles), Accessible Fiber diet colonized (A-HD, dark blue circles with outline), and Accessible Fiber diet non-colonized (A-NC, light blue circles). **B**, Redundancy analysis (RDA) of selected metabolites associated with diet and colonization, assessed using a Monte Carlo permutation test. Diet-associated metabolites are indicated for the Western diet (WD) and Accessible Fiber diet (AD), and metabolites influenced by *H. diminuta* colonization are shown as yellow markers. **C and D**, PCA plots illustrating metabolomic profiles stratified by colonization status within each dietary condition. Each point represents an individual sample ($n = 8$ per group). C shows separation between colonized and non-colonized rats under the Accessible Fiber diet, and D shows separation between colonized and non-colonized rats under the Western diet. Each data point represents one biological replicate (individual rat). In all panels, axes indicate the percentage of variance explained.

Fig. 9 | Impact of diet on cytokine gene expression in *Hymenolepis diminuta*-colonized and non-colonized rats.

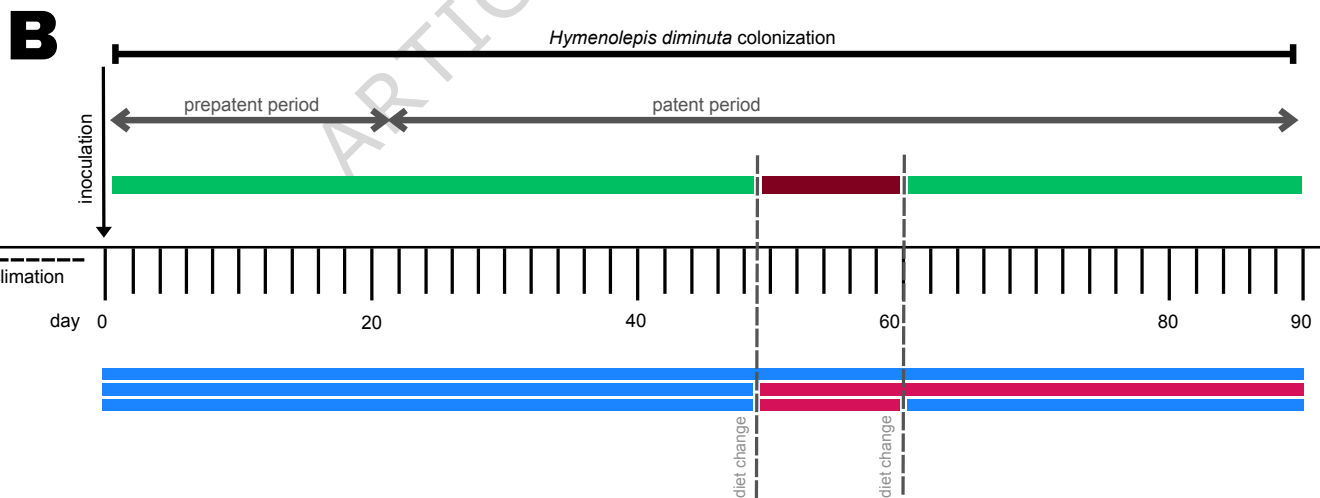
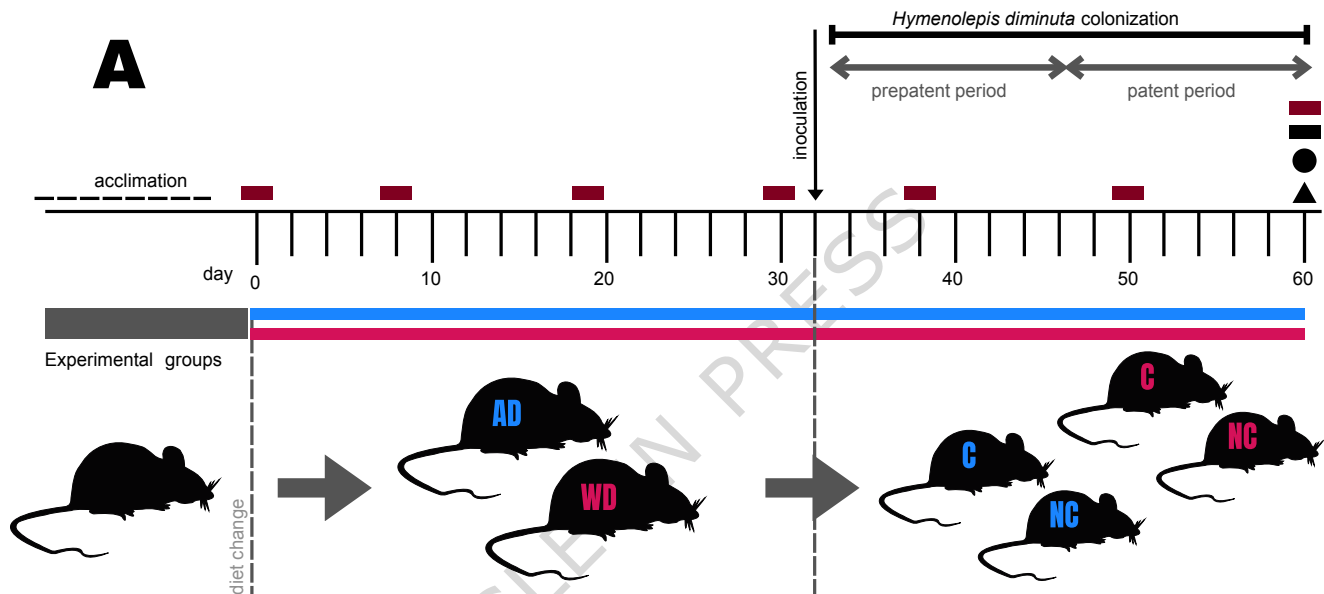
Relative expression of the cytokine genes *Il1b*, *Ifng*, *Il4* and *Il13* was quantified by qPCR in spleen tissue from Western-diet colonized (W-HD), Western-diet non-colonized (W-NC), Accessible Fiber–diet colonized (A-HD) and Accessible Fiber–diet non-colonized (A-NC) rats ($n = 8$ per group). All cytokine expression levels were normalized to the housekeeping gene *B2m*. Boxes represent the interquartile range (25th–75th percentiles) with the median indicated by the center line; whiskers extend to the minimum and maximum values, and dots denote individual rats. Group differences were analyzed using the two-sided Kruskal–Wallis test followed by Dunn's multiple comparisons test with adjustment for multiple testing. Each data point represents one biological

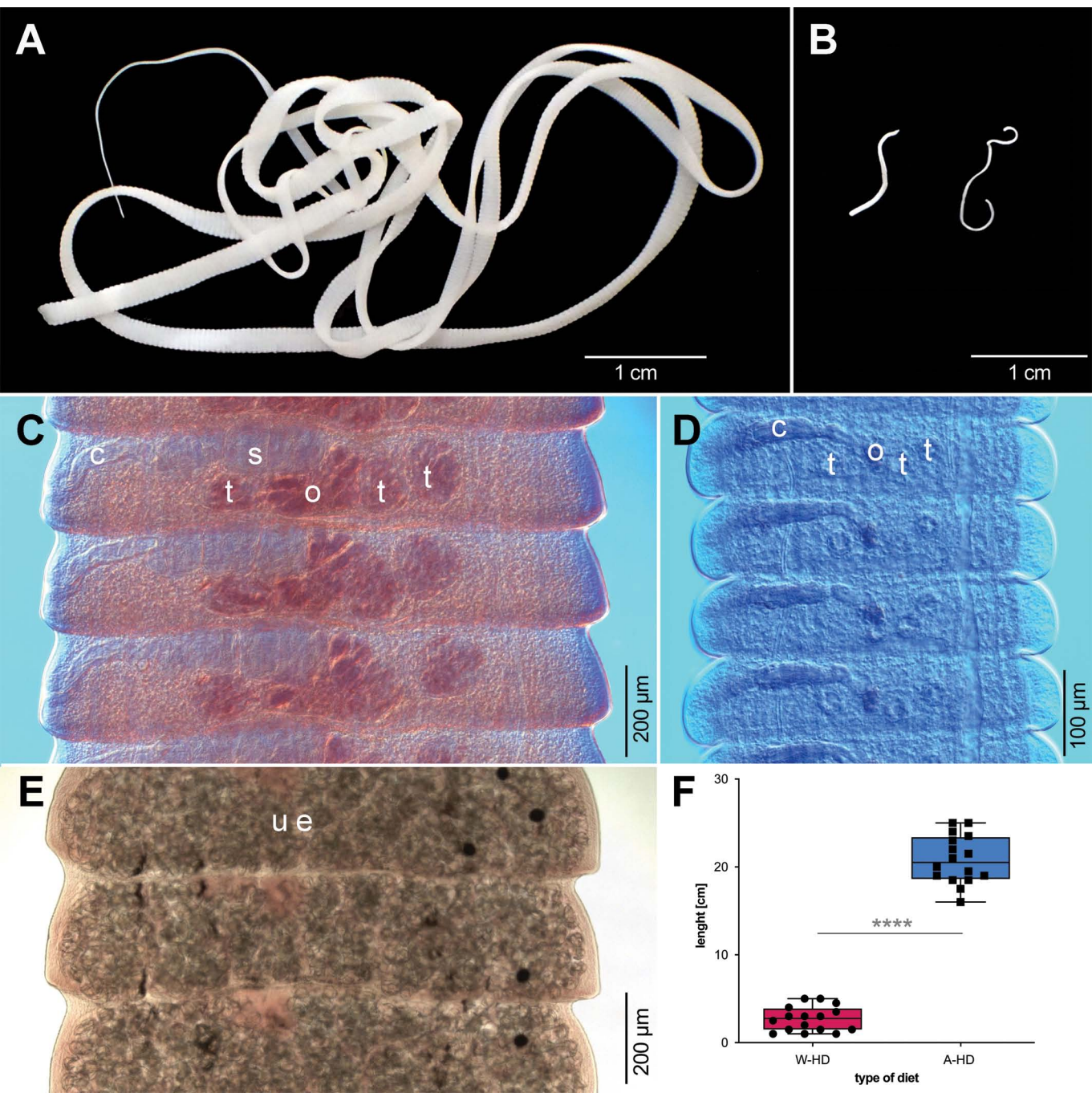
replicate (individual rat). Only statistically significant comparisons are indicated (*adjusted $p = 0.05$ – 0.01 , **adjusted $p = 0.01$ – 0.001 , ***adjusted $p < 0.001$).

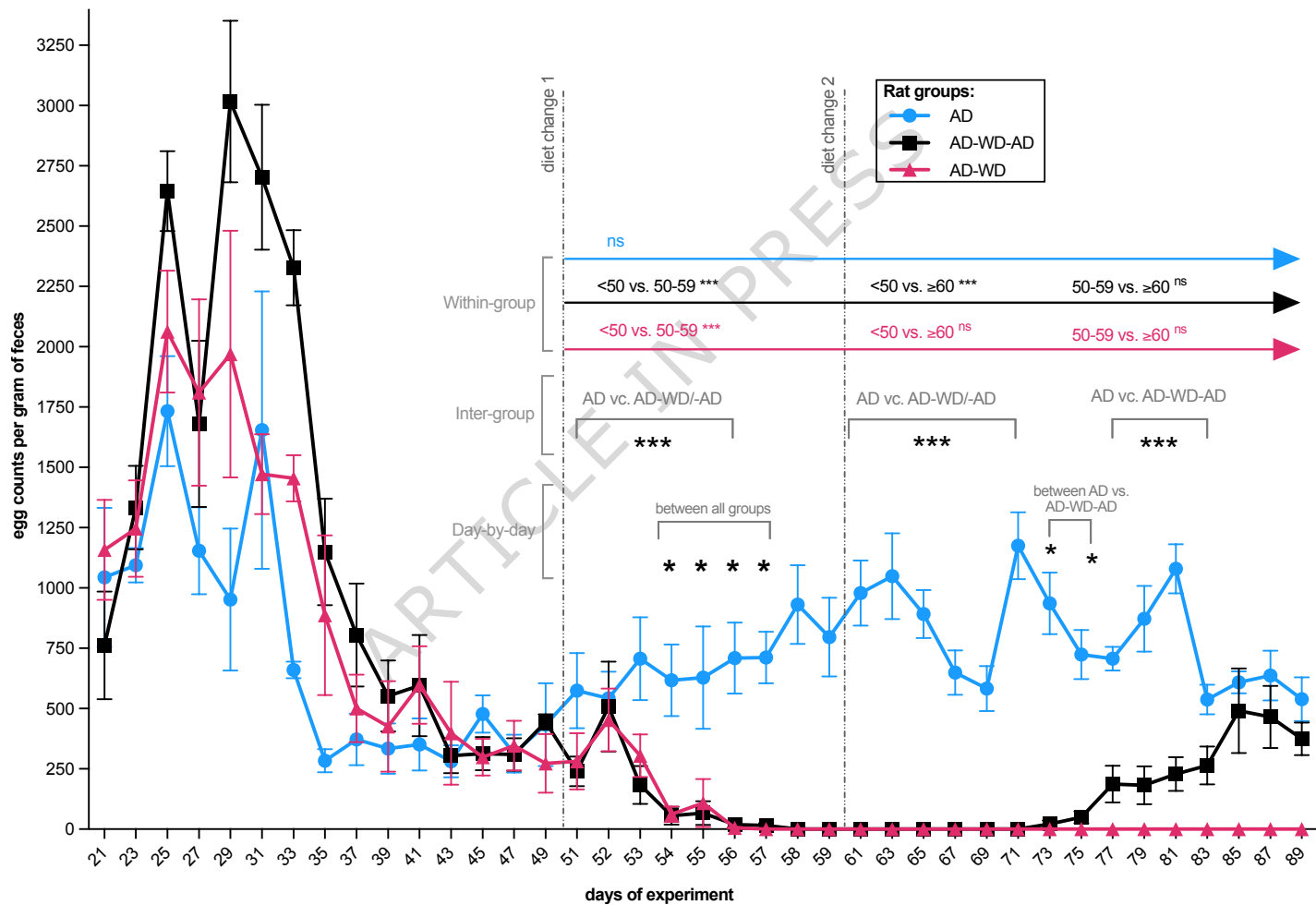
Here, the authors show that dietary fiber availability shapes the development and survival strategies of an intestinal worm, revealing stage-dependent plasticity and tight links between diet, the gut microbiome, host metabolism, and worm persistence.

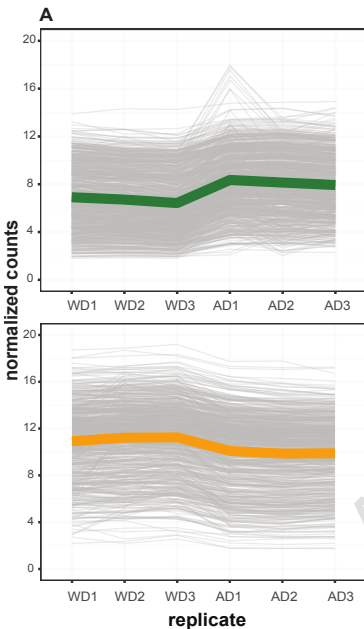
Peer Review Information: *Nature Communications* thanks the anonymous reviewers for their contribution to the peer review of this work. A peer review file is available.

ARTICLE IN PRESS









Down regulated
in Western Diet $n = 768$

Up regulated
in Western Diet $n = 691$

B**Biological Process**

Humoral response mediated by circulating immunoglobulin
Transport along microtubule & cytoskeleton-dependent intracellular transport
Somatic hypermutation of immunoglobulin genes

Cellular Process

Ciliary transition zone
Non-motile cilium
Centrosome
Stereocilia coupling link
Stereocilia tip link
Recombination nodule
Myosin VII complex
Egg and micropyle chrion

Molecular Process

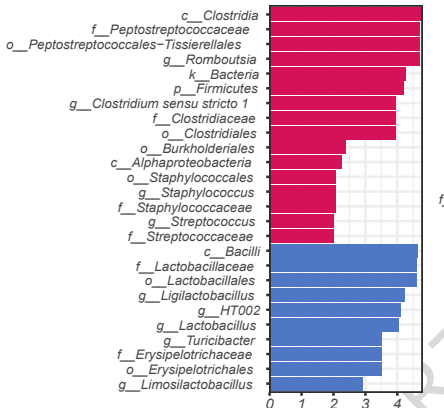
Protein binding
ATP-dependent activity, acting on DNA
Oxoglutarate dehydrogenase activity
Heparan sulfate proteoglykan binding protein
Ligase activity

Membrane (inner mitochondrial & platelet alpha granule)
Cytoplasmic vesicle lumen & secretory vesicles
Hemoglobin complex
Myelin & sperm fibrous sheath

DNA-binding transcription activator
Activity binding of ions receptor ligands, nucleoside, uracil, steroid & lipid
Cytokine activity
Carbohydrate transmembrane transporter activityL



A

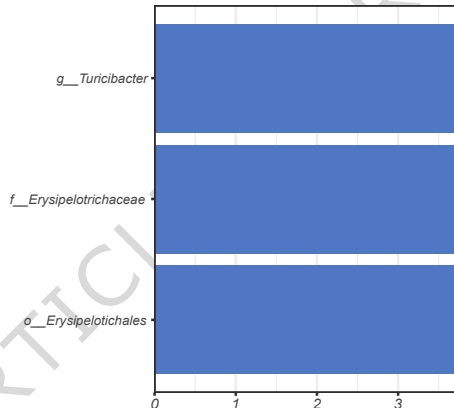


Enriched group

Accessible Fiber diet

Western diet

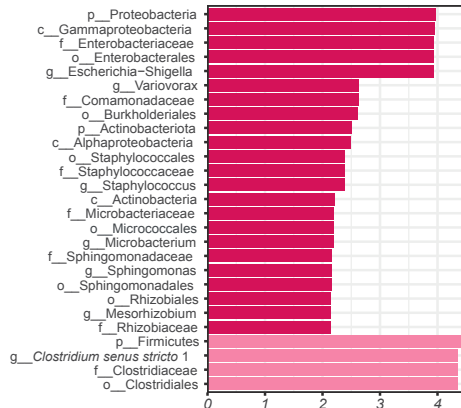
B



Enriched group

non-colonized

C



Enriched group

colonized

non-colonized

